Finite Element Analysis of Structure-acoustic Systems

Methods and Applications

Davidsson, Peter

2001

Document Version:
Publisher's PDF, also known as Version of record

LUND UNIVERSITY

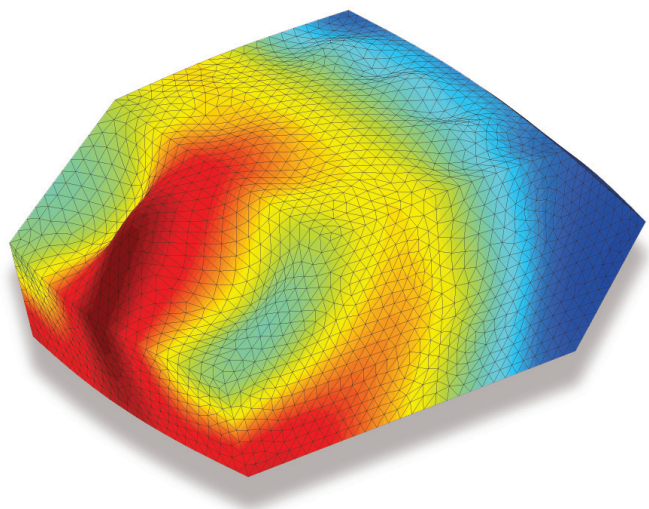

FINITE ELEMENT ANALYSIS OF STRUCTURE-ACOUSTIC SYSTEMS - Methods and Applications

PETER DAVIDSSON

Structural Mechanics

Licentiate Dissertation

Structural Mechanics

ISRN LUTVDG/TVSM--01/3060--SE (1-76)
ISSN 0281-6679

FINITE ELEMENT ANALYSIS OF STRUCTURE-ACOUSTIC SYSTEMS - Methods and Applications

PETER DAVIDSSON

Printed by KFS I Lund AB, Lund, Sweden, November, 2001.

For information, address:
Division of Structural Mechanics, LTH, Lund University, Box 118, SE-221 00 Lund, Sweden.
Homepage: http://www.byggmek.lth.se

Preface

The research presented in this licentiate thesis has been carried out at the Division of Structural Mechanics at Lund University. It is a part of the national research programme Integral Vehicle Structures (IVS) which concerns the development of future generations of vehicles. IVS is financed by the Swedish Foundation for Strategic Research (SSF).

I would like to thank my supervisor Prof. Göran Sandberg for his guidance and encouragement. I would also like to thank my good friends and colleagues at the Divisions of Structural Mechanics and Engineering Acoustics and express my gratitude for all the help they have provided and for the valuable discussions we have had. Special thanks to Lic. Ulf Nyman for our day-to-day discussions of research and many other things, and Mr. Bo Zadig for the help I have received in creating various of the figures.

Paper 3 presents work carried out in cooperation with Dr. Gunnar Björkman and M. Sc. Johan Svenningstorp at Volvo Technological Development in Göteborg. Their efforts to introduce me to the modelling environment described in the paper is gratefully acknowledged.

The research performed in Paper 4 was financed by Lindab Profil AB, I appreciate very much the interesting discussions I have had there with Lic. Hans Larsson and the enthusiasm he has shown.

Finally, I would like to thank Åsa for all her love and support.

Contents

Summary of papers

Paper 1 The problem in which a flexible structure interacts with an acoustic fluid is analysed by use of the finite element method. With increasing complexity of the geometry and when increasing the frequency limit is of interest, the number of degrees of freedom needed to describe the system becomes very large. To reduce the coupled system, modal analysis is performed in the structural and in the fluid domain separately. The uncoupled eigenvectors are then used to reduce the coupled problem. A method for choosing which uncoupled eigenvectors to include in this operation is derived, further reducing the system. A numerical example is provided, demonstrating the efficiency of the method.

Paper 2 The unsymmetrical eigenvalue problem involved in analysing structure-acoustic problems by use of the finite element method with a pressure formulation in the fluid domain can be reduced through transforming it into a symmetric standard eigenvalue problem. The paper shows that when hysteretic damping is introduced in both the structural and the fluid domain, the problem can still be treated as a symmetric standard eigenvalue problem, which becomes complex-valued due to the damping.

Paper 3 This paper, which is based on the results reported in Paper 1 and 2, describes the implementation of structure-acoustic finite element analysis in an integrated modelling environment, one which has interfaces to programs for meshing and for finite element analysis. The aim is to determine the vehicle interior noise on the basis of the force applied to the structure. An interface to a code developed for performing structure-acoustic analysis involving coupled modal analysis and frequency response analysis, is created. The possibilities this modelling environment provides are demonstrated. Use of this approach simplifies cooperation between researchers and their interaction with industrial groups.

Paper 4 Double leaf walls consisting of sheet-metal wall studs covered with plaster boards are studied. Acoustic behavior in the low frequency range is evaluated, aimed at determining the influence of the wall properties on sound reduction. The wall parameters studied are wall thickness, the number of plaster boards used, the stiffness of the wall stud web, and the boundary conditions. The influence of the dimensions of the connecting rooms is also studied. It is concluded that in the low frequency range the sound reduction a wall achieves can only be predicted by studying the actual room-wall-room configuration in question.

Introduction

Background

There is a constant aim of building lighter and more fuel efficient vehicles. The comfort of the passengers in terms of a low level of interior noise is in conflict with this, since the reduced weight increases the structural vibrations, which can lead to higher noise levels in the passenger compartment. To deal with this problem, detailed structure-acoustic analysis needs to be performed. In building acoustics the drive to use light weight constructions points in the same direction, having to face the same conflict. Simulation techniques to investigate such questions in advance are in great demand.
The finite element method is a well-established simulation tool for analysing complex structures. This is also the case for coupled structure-acoustic problems concerned with a flexible structure interacting with an acoustic fluid. Applications of such an approach in various fields of engineering are exemplified below.

Present work

The objective of this work has been to develop means for determining the interior noise level in a vehicle by use of structure-acoustic finite element analysis. The work involves use of a reduction technique in which the uncoupled modes of the structural and the fluid domain are used to reduce the size of the unsymmetrical coupled problem. A series of matrix transformations allows the coupled problem to be expressed as a reduced symmetric standard eigenvalue problem. A method was developed for choosing which uncoupled modes to include in this procedure further reducing the size of the coupled system. Damping is included in the analysis as a frequency independent loss factor for each domain. The reduction can be performed in the same fashion to obtain a complex valued symmetric standard eigenvalue problem. The results are implemented in an integrated modelling environment that simplifies future interaction with other research projects.
The computational methods developed are employed in a study of the acoustic behavior of light-weight double-leaf walls in the low frequency range. The aim is to increase the knowledge of how the wall properties influence the sound reduction caused by the wall.

Applications

The problem of a flexible structure interacting with an acoustic fluid is applicable to a wide range of engineering problems. Before presenting a mathematical account of the problem, a number of applications of the analysis procedure involved will be described briefly. Fig. 1 displays two vehicle applications. The first is the measurement setup used to determine the interior noise level in the SAAB 340 airplane. The second is a structure-acoustic analysis of the generic car cavity model developed in VIVS-lab. In Fig. 2, use of the finite element method for analysing the behavior within the low frequency range of a wall consisting of sheet-metal wall studs covered by plaster boards, is employed . Fig. 3 in turn shows a fluid-filled tank that has been exposed to an earthquake.

a)  b) 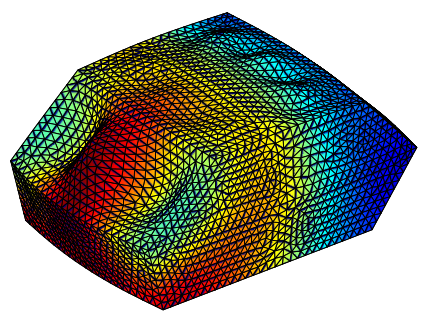

Figure 1: *Vehicle interior noise: a) Measurement setup for determining the level of interior noise in the SAAB 340 airplane (Tech. Lic. Mats Gustavsson, A2 Acoustics AB, project performed at SAAB AB during 1995), b) A coupled structure-acoustic mode of the vehicle model that was analysed in VIVS-lab (P. Davidsson, project with Volvo Technological Development, 2001).*

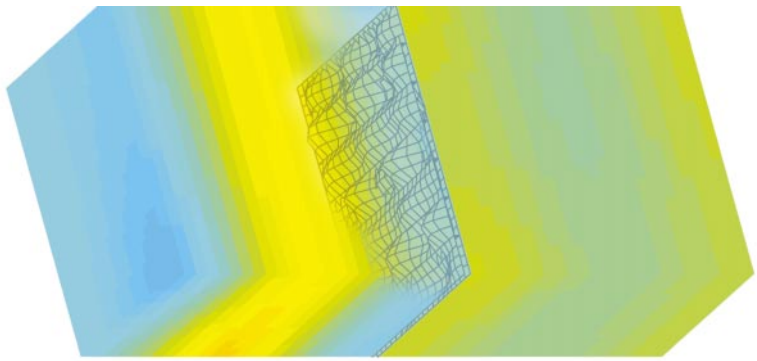

Figure 2: *Building acoustics: The acoustic behavior of double leaf walls is studied in the low frequency range. The figure shows the frequency response to a point source in the room-wall-room system simulating the measurement setup used for determining the sound reduction index of the wall (P. Davidsson, project together with Lindab Profil AB, 2001).*

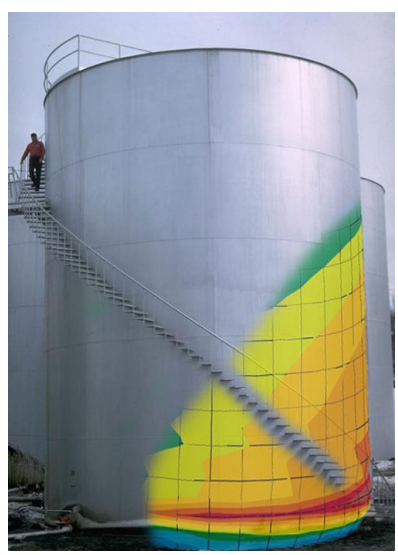

Figure 3: *Earthquake analysis: A fluid filled tank exposed to an earthquake, indicating damage typical, which is elephant foot buckling being seen at the base of the tank (P. Davidsson, Structural Mechanics, Report TVSM-5083, 1998).*

Structure-acoustic analysis

The finite element analysis of structure-acoustic systems has been the major concern of the thesis. As was shown in the previous section, the approach can be applied to a wide range of engineering problems. A detailed derivation of the basic theory can be found in [1, 2]. The finite element method has been employed in a number of studies [3, 4, 5, 6, 7, 8]. The governing equations are considered below, a finite element formulation of the coupled problem in which the pressure serves as the field variable in the fluid domain being derived.

Acoustic fluid

The following assumptions are made for a compressible fluid:

- The fluid is inviscid.
- The fluid is irrotational.
- The fluid only undergoes small displacements.

Three equations can be used to describe an acoustic fluid:
The equation of motion:

$$\rho_s \frac{\partial \mathbf{v}}{\partial t} + \nabla p_d = \rho_s \mathbf{b} \tag{1}$$

The continuity equation:

$$\frac{\partial \rho_d}{\partial t} + \rho_s \nabla \mathbf{v} = q \tag{2}$$

The constitutive equation:

$$p_d = c^2 \rho_d \tag{3}$$

Where $\mathbf{v} = \mathbf{v}(\mathbf{x}, t)$ is the velocity, $p_d = p_d(\mathbf{x}, t)$ the dynamic pressure, $\mathbf{b} = \mathbf{b}(\mathbf{x}, t)$ represents the body force. $\rho_d = \rho_d(\mathbf{x}, t)$ is the dynamic density, $q = q(\mathbf{x}, t)$ is the added fluid mass per unit volume. $\rho_s = \rho_s(\mathbf{x})$ is the static density and c is the speed of sound. The nonhomogeneous wave equation can be derived from Eqs. 1 - 3. Differentiating Eq. 2 with respect to time and using Eq. 3 provides

$$\frac{1}{c^2} \frac{\partial^2 p_d}{\partial^2 t} + \rho_s \nabla (\rho_s \frac{\partial \mathbf{v}}{\partial t}) = \frac{\partial q}{\partial t} \tag{4}$$

Substituting Eq. 1 into this expression provides the nonhomogeneous wave equation as expressed in terms of dynamic pressure p_d.

$$\frac{\partial^2 p_d}{\partial^2 t} - c^2 \nabla^2 p_d = c^2 \frac{\partial q}{\partial t} - c^2 \rho_s \nabla \mathbf{b} \tag{5}$$

From this point on the subscripts for dynamic pressure p_d and static density ρ_s are dropped. The boundary conditions applicable on the acoustic cavity are, rigid wall:

$$u_f|_n = -\frac{\partial p}{\partial n} = 0 \tag{6}$$

Impedance:

$$\frac{p}{v} = Z \tag{7}$$

Flexible wall:

$$u_s|_n = u_f|_n = -\frac{\partial p}{\partial n} \tag{8}$$

The finite element formulation of Eq. 5 can be derived by multiplying the equation by a test function, v, and integrating over a volume V

$$\int_V v\left(\frac{\partial^2 p}{\partial^2 t} - c^2\nabla^2 p - c^2\frac{\partial q}{\partial t} + c^2\rho\nabla\mathbf{b}\right)dV = 0 \tag{9}$$

Green's theorem provides the weak formulation

$$\int_V v\frac{\partial^2 p}{\partial^2 t}dV + c^2\int_V \nabla v\nabla p dV = c^2\int_A v\nabla p\mathbf{n}dA + c^2\int_V \frac{\partial q}{\partial t} - c^2\rho\nabla\mathbf{b}dV \tag{10}$$

The finite element method can be used to approximate the pressure field by

$$p = \mathbf{N}\mathbf{p} \tag{11}$$

where $\mathbf{N}$ contains the element shape functions and $\mathbf{p}$ the nodal pressures. Galerkin's method, employing the same shape functions, provides the weight functions

$$v = \mathbf{N}\mathbf{c} \tag{12}$$

Inserting this into Eq. 10 and noting that $\mathbf{c}$ is arbitrary yields the finite element formulation of the coupled problem

$$\int_V \mathbf{N}^T\mathbf{N}dV\ddot{\mathbf{p}} + c^2\int_V \nabla\mathbf{N}\nabla\mathbf{N}dV\mathbf{p} = c^2\int_A v\nabla p\mathbf{n}dA + c^2\int_V \frac{\partial q}{\partial t} - \rho\nabla\mathbf{b}dV \tag{13}$$

The following notation can then be employed

$$\mathbf{M}_f\ddot{\mathbf{p}} + \mathbf{K}_f\mathbf{p} = \mathbf{f}_q + \mathbf{f}_s \tag{14}$$

where

$$\mathbf{M}_f = \int_V \mathbf{N}^T\mathbf{N}dV \tag{15}$$

$$\mathbf{K}_f = c^2\int_V \nabla\mathbf{N}\nabla\mathbf{N}dV\mathbf{p} \tag{16}$$

$$\mathbf{f}_s = c^2 \int_A v \nabla p \mathbf{n} dA \tag{17}$$

$$\mathbf{f}_q = c^2 \int_V \frac{\partial q}{\partial t} dV \tag{18}$$

$$\mathbf{f}_{fb} = \int_V \rho \nabla \mathbf{b} dV \tag{19}$$

Structure

In most cases of interest the structural domain is a two-dimensional, such as a vibrating floor panel in a vehicle, for example. This can be described by use of plate or shell theory, see [8, 9] for finite element formulation of these types of problems. The finite element formulation of the structure also results in an equation system of motion

$$\mathbf{M}_s \ddot{\mathbf{d}} + \mathbf{K}_s \mathbf{d} = \mathbf{f}_b + \mathbf{f}_q \tag{20}$$

where $\mathbf{d}$ denotes the nodal displacements. The force term due to distributed loading $\mathbf{f}_q$ can be divided into two parts, one dealing with the forces that are distributed. The other deals with the coupling to the fluid domain through the fluid pressure that acts on the structure

$$\mathbf{f}_f = \int_S \mathbf{N}_s^T (p(\mathbf{r}, t)\mathbf{n}) dS \tag{21}$$

where $\mathbf{N}_s$ denotes the structural shape functions, p the fluid pressure and $\mathbf{n}$ the normal vector pointing out of the fluid domain.

A finite element formulation of the coupled system

The structure-acoustic fluid coupling is introduced as force terms at the boundary, S, between the two domains, Eq. 17 and 21. At this boundary the fluid particles and the structure move together. The boundary condition becomes

$$\mathbf{u}_s \mathbf{n}|_S = \mathbf{u}_f \mathbf{n}|_S \tag{22}$$

Using the relation between pressure and acceleration in the fluid domain

$$\nabla p(\mathbf{r}, t) = -\rho \frac{\partial^2 \mathbf{u}_f(\mathbf{r}, t)}{\partial t^2} \tag{23}$$

the force acting on the fluid can be described in terms of structural acceleration

$$\nabla p(\mathbf{r}, t)|_S = -\rho \frac{\partial^2 \mathbf{u}_f(\mathbf{r}, t)}{\partial t^2}|_S = -\rho \frac{\partial^2 \mathbf{u}_s(\mathbf{r}, t)}{\partial t^2}|_S \approx -\rho \mathbf{n}^T \mathbf{N}_s \ddot{\mathbf{d}} \tag{24}$$

The finite element approximation of the structural acceleration is used in the last step. The introduction of a coupling matrix

$$\mathbf{H} = \int_S \mathbf{N}_s^T \mathbf{n} \mathbf{N}_f dS \tag{25}$$

allows the coupling forces to be written as

$$\mathbf{f}_f = \int_S \mathbf{N}_s^T \mathbf{n} \mathbf{N}_f dS \mathbf{p} = \mathbf{H}\mathbf{p} \tag{26}$$

and

$$\mathbf{f}_s = -\rho c^2 \int_S \mathbf{N}_f^T \mathbf{n}^T \mathbf{N}_s dS \ddot{\mathbf{d}} = -\rho c^2 \mathbf{H}^T \ddot{\mathbf{d}} \tag{27}$$

The structure-acoustic problem can then be described by an unsymmetrical equation system

$$\begin{bmatrix} \mathbf{M}_s & \mathbf{0} \\ \rho c^2 \mathbf{H}^T & \mathbf{M}_f \end{bmatrix} \begin{bmatrix} \ddot{\mathbf{d}} \\ \ddot{\mathbf{p}} \end{bmatrix} + \begin{bmatrix} \mathbf{K}_s & -\mathbf{H} \\ 0 & \mathbf{K}_f \end{bmatrix} \begin{bmatrix} \mathbf{d} \\ \mathbf{p} \end{bmatrix} = \begin{bmatrix} \mathbf{f}_b \\ \mathbf{f}_q \end{bmatrix} \tag{28}$$

This system is the basis for all analyses performed in the thesis.

References

[1] F. Fahy, Sound and Structural Vibration (Academic Press 1985).

[2] L. Cremer, M. Heckl, Structure-Bourne Sound (Second Edition, Springer-Verlag 1988).

[3] G. Sandberg, Finite Element Modelling of Fluid-Structure Interaction, Doctoral Thesis, Division of Structural Mechanics at Lund Institute of Technology, Sweden (1986).

[4] H. Carlsson, Finite Element Analysis of Structure-Acoustic systems; Formulations and Solution Strategies, Doctoral Thesis, Division of Structural Mechanics at Lund Institute of Technology, Sweden (1992).

[5] M. Gustavsson, Methods for Aircraft Noise and Vibration Analysis, Licensiate Thesis, Division of Structural Mechanics at Lund Institute of Technology, Sweden (1998).

[6] P. A. Hansson, Finite Element Analysis of Fluid-Structure Systems; Element Formulations and Decomposition Strategies, Licensiate Thesis, Division of Structural Mechanics at Lund Institute of Technology, Sweden (1999).

[7] H. J.-P. Morand, R. Ohayon, Fluid Structure Interaction (John Wiley & Sons 1995).

[8] O. C. Zienkiewicz, R. L. Taylor, The Finite Element Method, Volume 2 (McGraw-Hill Book Company 1991).

[9] K. J. Bathe, Finite Element Procedures (Prentice-Hall 1996).

Paper 1

Choosing modes in the reduction of structure-acoustic systems

Göran Sandberg, Peter Davidsson
Division of Structural Mechanics
Lund Institute of Technology

Choosing modes in the reduction of structure-acoustic systems

Göran Sandberg, Peter Davidsson
Division of Structural Mechanics, Lund University, Sweden

Abstract

Methods for choosing a modal basis for the reduction of structure-acoustic systems based on the finite element method are investigated. The coupled system is set up using a displacement formulation in the structural domain and a pressure formulation in the fluid domain, resulting in an unsymmetrical system. This system is reduced by the uncoupled modes of the two subdomains. The paper proposes methods for choosing which of these modes to include in the reduced model by evaluating the characteristics of the coupling between the modes of the two domains. Uncoupled modes with strong coupling that depends on similarity in the natural frequencies or in the mode shapes are included in the reduction. A numerical example is given for verifying the methods proposed.

1 Introduction

The coupled problem of a structure interacting with an acoustic fluid is of interest in many fields of engineering. It can concern a fluid-filled tank exposed to an earthquake or the noise level due to structural vibrations in a vehicle compartment. In the case studied here the fluid domain is an enclosed one and is assumed to be both inviscid and irrotational and the motions involved are small. Many different formulations for describing the structure-acoustic problem have been proposed by Ref. [1, 2, 3, 4]. In the present paper the nodal variable in the structural domain is displacement and in the fluid domain pressure. Using a finite element formulation gives an unsymmetrical equation system, the lack of symmetry being due to the coupling terms between the structural domain and the fluid domain. Problems involving structure-fluid interaction typically generate very large systems of equations. In performing modal analysis, the system can be reduced by using the uncoupled modes of the two domains [5, 6]. The system can also be made symmetric by matrix

transformations [7, 8, 9]. The coupled modes are dominated by either the structure or the fluid, each uncoupled mode providing a corresponding coupled mode. The need for only including a selected portion of the uncloupled modes in the reduction of the coupled problem is stated in [5]. In [10] a possible way of choosing coupling modes is outlined. In the present paper, a method, also proposed in [11] is used for determining which uncoupled modes of the two domains are strongly coupled. By including only these in the reduction of the coupled problem the equation system of interest can be reduced further. A numerical example is presented based on the work described in [12] where the structure-acoustic behavior of an aircraft fuselage was studied. The paper elaborates on the importance of a correct choice of modal basis in structure-acoustic calculations and obtaining a proper understanding of the coupling phenomena which link the two domains.

2 Finite element formulation

The governing equation for the fluid here is the acoustic equation

$$\frac{\partial^2 p}{\partial t^2} - c^2 \nabla^2 p = c^2 \frac{\partial q}{\partial t} \tag{1}$$

whereas the governing equation for the structure can be written as an operator acting on the displacement field

$$\mathtt{L}(u_s) = F_s(\mathbf{r}, t) \tag{2}$$

A finite element formulation of the governing equations gives the equations of motion both in the structural domain

$$\mathbf{M}_s \ddot{\mathbf{d}} + \mathbf{K}_s \mathbf{d} = \mathbf{f}_b + \mathbf{f}_f \tag{3}$$

where $\mathbf{d}$ denotes the nodal displacements, and in the fluid domain

$$\mathbf{M}_f \ddot{\mathbf{p}} + \mathbf{K}_f \mathbf{p} = \mathbf{f}_q + \mathbf{f}_s \tag{4}$$

where $\mathbf{p}$ is the pressure. For a further account of the system matrices see [7].
In both Eq. (3) and (4), the term $\mathbf{f}_f$ and $\mathbf{f}_s$ represent the coupling between the structural domain and fluid domain. The structure is subjected to a force at the boundary between the domains due to the fluid pressure normal to the boundary surface.

$$\mathbf{f}_f = \int_S \mathbf{N}_s^T (p(\mathbf{r}, t)\mathbf{n}) dS \tag{5}$$

where $\mathbf{r} = (x, y, z)$. $\mathbf{n} = [n_x\ n_y\ n_z]^T$ is the boundary surface normal and $\mathbf{N}_s$ denotes the structural shape functions. The force acting on the fluid due to displacement of the structure can be derived from

$$\mathbf{f}_s = c^2 \int_S \mathbf{N}_f^T (\nabla p(\mathbf{r}, t)\mathbf{n}) dS \tag{6}$$

where $\nabla = [\partial/\partial x\ \partial/\partial y\ \partial/\partial z]^T$ and $\mathbf{N}_f$ is the fluid shape functions. In the fluid domain the relation between pressure and acceleration is

$$\nabla p(\mathbf{r}, t) = -\rho \frac{\partial^2 \mathbf{u}_f(\mathbf{r}, t)}{\partial t^2} \tag{7}$$

At the connecting boundary the movement of the two domains in the normal direction is equal to

$$\mathbf{u}_s \mathbf{n}|_S = \mathbf{u}_f \mathbf{n}|_S \tag{8}$$

This enables the force acting on the fluid due to structural movement to be written in terms of structural acceleration.

$$\nabla p(\mathbf{r}, t)|_S = -\rho \frac{\partial^2 \mathbf{u}_f(\mathbf{r}, t)}{\partial t^2}|_S = -\rho \frac{\partial^2 \mathbf{u}_s(\mathbf{r}, t)}{\partial t^2}|_S \approx -\rho \mathbf{n}^T \mathbf{N}_s \ddot{\mathbf{d}} \tag{9}$$

In the final step the structural accelerations are approximated by a finite element formulation. Using this to express $\mathbf{f}_s$ gives

$$\mathbf{f}_s = -\rho c^2 \int_S \mathbf{N}_f^T \mathbf{n}^T \mathbf{N}_s dS \ddot{\mathbf{d}} = -\rho c^2 \mathbf{H}^T \ddot{\mathbf{d}} \tag{10}$$

The coupling matrix $\mathbf{H}$ that is introduced can also be used to describe $\mathbf{f}_f$

$$\mathbf{f}_f = \int_S \mathbf{N}_s^T \mathbf{n} \mathbf{N}_f dS \mathbf{p} = \mathbf{H}\mathbf{p} \tag{11}$$

Eqs. (3) and (4) can now be written in matrix form to yield the following equation system:

$$\begin{bmatrix} \mathbf{M}_s & \mathbf{0} \\ \rho c^2 \mathbf{H}^T & \mathbf{M}_f \end{bmatrix} \begin{bmatrix} \ddot{\mathbf{d}} \\ \ddot{\mathbf{p}} \end{bmatrix} + \begin{bmatrix} \mathbf{K}_s & -\mathbf{H} \\ 0 & \mathbf{K}_f \end{bmatrix} \begin{bmatrix} \mathbf{d} \\ \mathbf{p} \end{bmatrix} = \begin{bmatrix} \mathbf{f}_b \\ \mathbf{f}_q \end{bmatrix} \tag{12}$$

The coupling matrix $\mathbf{H}$ makes the system matrices unsymmetrical and therefore both the left and right eigenvectors need to be calculated in order to diagonalise the system. $\mathbf{H}$ is used for choosing which uncoupled structural and fluid modes to include in the coupled analysis.

3 Modal reduction

The procedure for establishing a symmetric system of equations has been described in a previous paper, Ref. [7]. The eigenmodes of the subdomains are first calculated according to

$$\begin{aligned} \Phi_s^T \mathbf{M}_s \Phi_s &= \mathbf{I}_s & \Phi_s^T \mathbf{K}_s \Phi_s &= \mathbf{D}_s \\ \Phi_f^T \mathbf{M}_f \Phi_f &= \mathbf{I}_f & \Phi_f^T \mathbf{K}_f \Phi_f &= \mathbf{D}_f \end{aligned} \tag{13}$$

where Φ_s and Φ_f are eigenvectors of the structural and the fluid domain, respectively. $\mathbf{D}_s$ and $\mathbf{D}_f$ contain the eigenvalues of the two domains in the diagonal. On the basis of these eigenmodes, the coupled system can be reformulated according to Eq. (12). The final result of this operation is

$$\begin{bmatrix} \ddot{\zeta}_s \\ \ddot{\zeta}_f \end{bmatrix} + \begin{bmatrix} \mathbf{D}_s & -\sqrt{\rho c^2}\sqrt{\mathbf{D}_s}\Phi_s^T \mathbf{H} \Phi_f \\ -\sqrt{\rho c^2}\Phi_f^T \mathbf{H}^T \Phi_s \sqrt{\mathbf{D}_s} & \mathbf{D}_f + \rho c^2 \Phi_f^T \mathbf{H}^T \Phi_s \Phi_s^T \mathbf{H} \Phi_f \end{bmatrix} \begin{bmatrix} \zeta_s \\ \zeta_f \end{bmatrix} = \begin{bmatrix} \sqrt{\rho c^2}\sqrt{\mathbf{D}_s}\Phi_s^T \mathbf{f}_b \\ \Phi_f^T \mathbf{f}_q - \rho c^2 \Phi_f^T \mathbf{H}^T \Phi_s \Phi_s^T \mathbf{f}_b \end{bmatrix} \tag{14}$$

which gives the right eigenvectors. Setting up a system with the transposed system matrices gives the left eigenvectors.

4 Choosing uncoupled modes.

The reduced coupled system of equations for the structure acoustic fluid interaction problem is given in Eq. (14) where the uncoupled modes of the two domains are used in the final representation. The eigenmodes of the coupled problem below a certain frequency are required. If the contribution of each uncoupled mode to the coupled solution can be determined only the most important ones need to be included in the reduced model.

The influence of the uncoupled modes on the natural frequency of the coupled solution using one mode from each subdomain, is elaborated in [13]. The eigenpair for the structure is $<\psi_{si}^n, \omega_{si}>$ where n stands for displacement normal to the surface, and for the fluid is $<\psi_{fj}, \omega_{fj}>$. The natural frequency of the coupled system is influenced by the similarity in natural frequency between ω_{si} and ω_{fj} and the dimensionless spatial coupling coefficient C_{ij} being given by

$$C_{ij} = \frac{1}{S} \int_S \psi_{si}^n \psi_{fj} dS \tag{15}$$

where S is the connecting area between the structural domain and fluid domain. When the two uncoupled natural frequencies are equal $\omega_{si} = \omega_{fj}$ the interaction is

equivalent to the behavior of an auxiliary mass-spring system on a primary oscillator. One of the corresponding natural frequencies of the coupled system is larger and the other is smaller than the uncoupled one. When $\omega_{si} \gg \omega_{fj}$ or $\omega_{si} \ll \omega_{fj}$ the natural frequencies of the coupled modes are only changed on the basis of similarity in the mode shapes.
From this brief discussion and the references it can be concluded that in using uncoupled modes in the reduction the similarity between the uncoupled natural frequencies, ω_{si} and ω_{fj}, as well as the size of the coefficient C_{ij} determine the influence of each of these uncoupled modes on the coupled modes. The aim of the paper is to propose a method for using this information to determine which uncoupled modes are important and to only include them in the subsequent reduction of the coupled problem. To this end, the method discussed in [11] can be employed. The method involves coupling by means of the mode shapes and the natural frequencies of the two domains, using the expression

$$B_{ij} = \frac{\Phi_{si}^T \mathbf{H} \Phi_{fj}}{(1 + i\xi_{sj})\omega_{sj}^2 - (1 + i\xi_{ai})\omega_{ai}^2} \tag{16}$$

This expression allows the coupling between the structural domain and the fluid domain to be determined creating the possibility of choosing the most important uncoupled modes to include in the reduced coupled problem. In the undamped case

$$B_{ij} = \frac{\Phi_{si}^T \mathbf{H} \Phi_{fj}}{\omega_{sj}^2 - \omega_{ai}^2} \tag{17}$$

The numerator corresponds to the coefficient C_{ij} in Eq. (15). In the denominator, natural frequencies of the i'th structural mode and the j'th fluid mode are introduced, similar frequencies giving a value close to zero. Similarity in the mode shapes and similarity in the natural frequencies gives a large value for B_{ij}, the corresponding modes being included in the coupled analysis. The following variables are defined, see also Fig. 1:

Φ_s denotes all available uncoupled structural modes. n_s being the number of these modes
Φ_f denotes all available uncoupled fluid modes. n_f being the number of these modes
$\hat{\Phi}_s = \{\Phi_{si} \in \Phi_s; \omega_{si} \leq \hat{\omega}\}$
$\hat{\Phi}_f = \{\Phi_{fi} \in \Phi_f; \omega_{fi} \leq \hat{\omega}\}$

where $\hat{\omega} = 2\pi\hat{f}$ and $\hat{f}$ is the highest frequency of interest.
The scheme for choosing which uncoupled modes to include in the analysis is as follows:

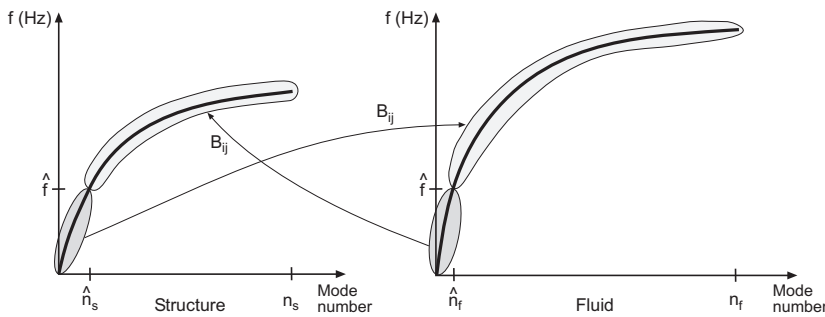

Figure 1: *Natural frequencies of the two domains plotted against the mode number. Uncoupled modes of the two domains are compared using Eq. (17) and the most important modes to describe the coupled system can be included in the reduced coupled analysis, Eq. (14).*

1. Perform modal analyses of the uncoupled structural and fluid domains, calculating Φ_s and Φ_f.

2. On the basis of the maximum frequency of interest, $\hat{f}$, determine $\hat{\Phi}_s$ and $\hat{\Phi}_f$. All of these modes are included in the reduction of the coupled problem.

3. Determine the coupling between $\hat{\Phi}_s$ and Φ_f using Eq. (17). The number n_{coup} of fluid modes with the strongest coupling for each structural mode is determined. These fluid modes above the frequency range of interest are also included in the reduction, see Figure 1. The effect of the value of n_{coup} is studied in the numerical example.

4. Use the same method for the fluid modes $\hat{\Phi}_f$ comparing them with Φ_s for determining which structural modes above the frequency range of interest should be included in the reduction.

5. Perform the reduced coupled modal analysis, based on Eq. (14), using the structural and fluid modes chosen.

Since all the modes below the frequency limit $\hat{f}$ are included the numerator has only a small effect on the choice of modes in the upper frequency range, assuming that the condition $\omega_{si} \gg \omega_{fj}$ or $\omega_{si} \ll \omega_{fj}$ is satisfied. Instead of using Eq. (17) a simplified expression

$$\hat{\mathbf{B}} = \Phi_s^T \mathbf{H} \Phi_f \tag{18}$$

in which only the similarity in mode shapes is calculated, can be used to determine the modes to include in the analysis. These two methods, method I represented by Eq. (17) and method II represented by Eq. (18), are evaluated in the numerical example in the next section.

5 Numerical example

5.1 Model

In this section the two methods for choosing modes described above are evaluated. The number of uncoupled modes needed for describing the coupled system is examined. A simple three-dimensional body is analysed, Figure 2. The model employed is based on [12], in which numerical and experimental work has been performed. It involves a cylindrical steel shell 1.2 mm thick with a 0.183 m radius. Circular aluminum plates 25.4 mm thick are attached to the ends of the cylinder. The material properties are listed in Table 1 and the number of degrees-of-freedom for the domains being shown in Table 2. Modal analysis of the fluid domain and the structural domain is performed by MSC/Nastran [14] and the coupled modal analysis by Matlab/CALFEM [15]. The results are compared with a direct solution of the unsymmetrical coupled problem using MSC/Nastran. In total, 500 modes are calculated for the structure, Φ_s, and 1000 modes are calculated for the fluid, Φ_f. The reduction process for the coupled problem is based on these modes. The total number of uncoupled modes needed to describe the coupled system is evaluated. The methods described for choosing modes are studied by varying the number of uncoupled modes with strong coupling that are included, i.e. the number n_{coup}. The mode shapes calculated, $\mathbf{\Phi}_{reduced}$, are compared with the modes obtained in solving the total system, $\mathbf{\Phi}_{total}$, using the expression

$$\kappa = \frac{\mathbf{\Phi}_{reduced}^T \cdot \mathbf{\Phi}_{total}}{|\mathbf{\Phi}_{reduced}| \cdot |\mathbf{\Phi}_{total}|} \tag{19}$$

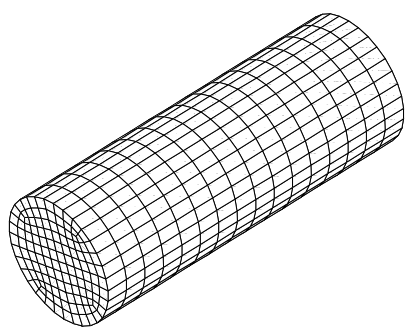

Figure 2: *Finite element model of the three-dimensional body.*

Table 1: *Material data for the body.*

Steel:	E	=	210	GPa
	ν	=	0.30	
	ρ	=	7800	kg/m^3
Aluminum:	E	=	70	GPa
	ν	=	0.30	
	ρ	=	2700	kg/m^3
Air:	ρ	=	1.21	kg/m^3
	c	=	340	m/s.

The value of κ is between 0 to 1 where 1 represents exact agreement between the modes that are compared.

5.2 Coupled analysis without choosing modes

The effect of the number of uncoupled structural modes, n_s, and fluid modes, n_f, included in the analysis is shown in Figure 3. The maximum frequency of interest is set to 500 Hz, the similarity between the reduced model and the total model, κ, being plotted for the 22 coupled modes with natural frequency below this value. Four cases are shown in the figure, differing in the number of uncoupled modes included, namely: 1) all uncoupled modes up to 1.2 times the highest frequency of interest, which gives $n_s = 39, n_f = 9$ ($\circ$); 2) $n_s = 100, n_f = 200$ ($*$); 3) $n_s = 200, n_f = 500$ ($\triangle$); 4) $n_s = 500, n_f = 1000$ ($\times$). Note that in this case all the modes are employed. The similarity in mode shapes is plotted for the structural and fluid parts of the coupled eigenvector separately. For the structural part of the mode the shape is exact for those modes dominated by the structure. In contrast, modes 1 and 15 are dominated by the fluid. Thus, a large number of structural modes are needed to describe the behavior of the coupled modes. The same is true for the fluid domain, where the modes dominated by the fluid are represented exactly. From this it is obvious that many of the uncoupled modes do not contribute to the coupled solution

Table 2: *Finite element model data.*

Domain	Degrees-of-freedom
Structure	4620
Acoustic fluid	2465
Total	7085

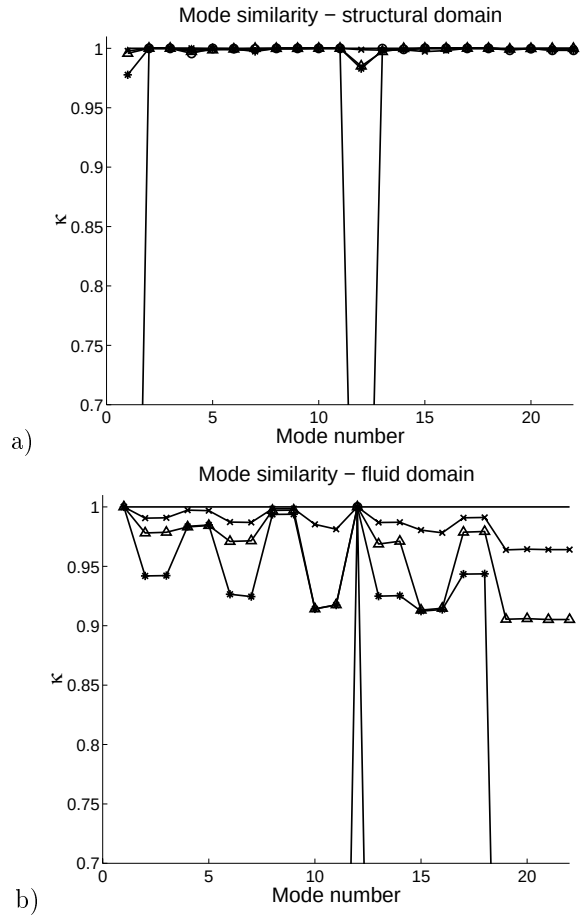

Figure 3: *Similarity between modes in the reduced model and in the total model: a) structural part, b) fluid part. Modes included:* $n_s = 39, n_f = 9$*, all uncoupled modes with a natural frequency of up to 600 Hz* ($\circ$)*;* $n_s = 100, n_f = 200$ ($*$)*;* $n_s = 200, n_f = 500$ ($\triangle$)*;* $n_s = 500, n_f = 1000$ ($\times$)

and can thus be sorted out. When the 22 lowest coupled modes are calculated, based on originally 500 structural modes and 1000 fluid modes, the minimum values are $\kappa = 0.997$ for the structure and $\kappa = 0.964$ for the fluid.

5.3 Proposed method

The methods for selecting modes are evaluated by making selections from the 500 structural modes, Φ_s, and the 1000 fluid modes, Φ_f, that are lowest. Since the highest frequency of interest is 500 Hz, $\hat{\Phi}_s$ represents the 26 lowest structural modes (including 6 zero-modes). $\hat{\Phi}_f$ represents the 3 lowest fluid modes (including one zero-mode).
Figure 4 displays the similarity in mode shapes for each domain as obtained for method I when n_{coup}, according to the suggested scheme, is increased from one to twenty. The mean and the minimum value of κ for the first 22 coupled modes (below 500 Hz) are displayed for the structural and the fluid part of the coupled eigenvector separately. The horizontal dotted lines are the minimum κ which is obtained when all 500 structural and 1000 fluid modes are included. In Figure 5 the corresponding number of uncoupled modes included in the coupled analysis is plotted. The results for method II are displayed in Figures 6 and 7. Note that all the modes below 500 Hz from each subdomain are included in the final analysis. The selection of modes above this frequency is based on the degree to which they interact with the modes below this frequency in the other domain. The first method provides very close agreement for $n_{coup} = 11$, where 236 uncoupled modes (42 structural and 194 fluid modes) are included in the coupled analysis. The number of degrees-of-freedom for the coupled system is thus reduced from 7085 to 236, with very high accuracy being maintained. The eigenvalue problem is also of a standard symmetric form which makes it easy to solve. The second method which uses a simpler method, also yields good results, but since the frequency dependence is neglected a less smooth curve of convergence is obtained.

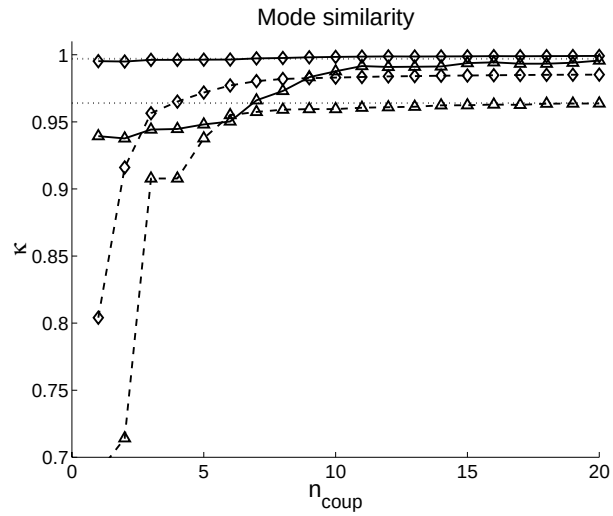

Figure 4: *Method I (Eq. 17). Similarity between modes in the reduced model and in the total model: Solid line - structural domain. Dashed line - fluid domain.* △ *- minimum value of* κ*,* ◇ *- mean value of* κ*.*

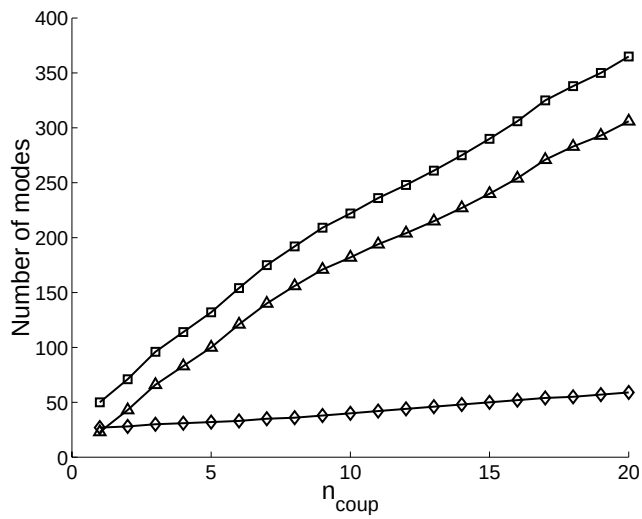

Figure 5: *Method I (Eq. 17). Number of modes from the subdomains included:* ◇ *- structural domain,* △ *- fluid domain,* □ *- Total number.*

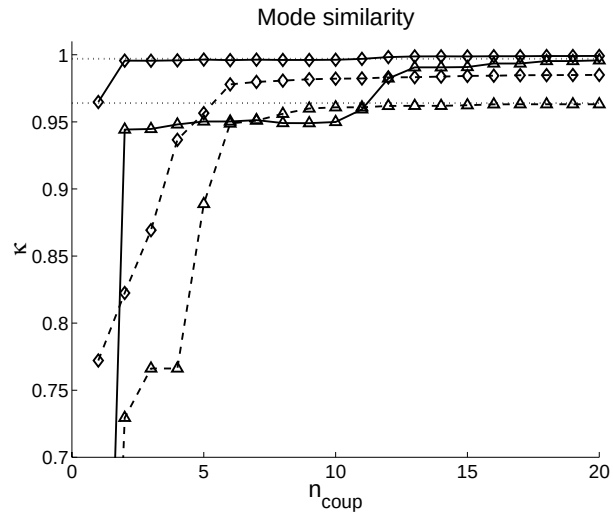

Figure 6: *Method II (Eq. 18). Similarity between modes in the reduced model and in the total model: Solid line - structural domain. Dashed line - fluid domain.* △ *- minimum value of* κ*,* ◇ *- mean value of* κ*.*

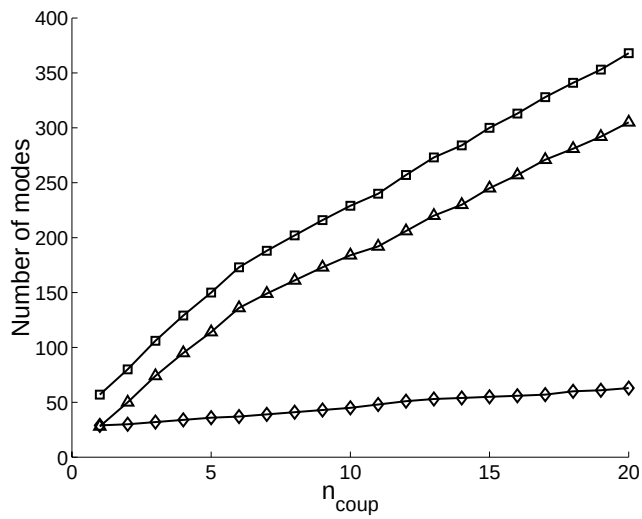

Figure 7: *Method II (Eq. 18). Number of modes from the subdomains included:* ◇ *- structural domain,* △ *- fluid domain,* □ *- Total number.*

6 Conclusions

A structure-acoustic system is analysed here, using a strategy for substructuring and reducing the coupled problem by using the uncoupled modes of the structural and the fluid domains. Since a large number of modes from the subdomains is needed to describe the coupled system, a method for choosing uncoupled modes that contribute most strongly to a description of the coupled problem in the frequency range of interest is studied. The paper proposes two methods which are similar, Method I involves selecting the uncoupled modes on the basis of strong coupling using resemblance in terms both of frequency and of mode shapes. Method II involves determining the most important uncoupled modes on the basis of the similarity in mode shapes only. The numerical example shows Method I to give the best results. That method allows the coupled system to be reduced from 7085 to 236 degrees-of-freedom, with only a small loss of accuracy. The reduced system is symmetric. Comparing the results for the reduced system using a selected set of modes with those obtained using all the modes available shows the results to be almost identical. For the case analysed here the number of modes included is reduced from 1500 to 236.

References

[1] O. C. Zienkiewicz, R. L. Taylor, The Finite Element Method, Volume 2 (McGraw-Hill Book Company 1991).

[2] G. Sandberg, Finite Element Modelling of Fluid-Structure Interaction, Doctoral Thesis, Division of Structural Mechanics at Lund Institute of Technology, Sweden (1986).

[3] H. Carlsson, Finite Element Analysis of Structure-Acoustic systems; Formulations and Solution Strategies, Doctoral Thesis, Division of Structural Mechanics at Lund Institute of Technology, Sweden (1992).

[4] H. J.-P. Morand, R. Ohayon, Fluid Structure Interaction (John Wiley & Sons 1995).

[5] J. A. Wolf JR, Modal Synthesis for Combined Structural-Acoustic Systems, AIAA Journal, 15(5) (1977) 743-745.

[6] D. J. Nefske, J. A. Wolf JR, L. J. Howell, Structural-Acoustic Finite Element Analysis of the Automobile Passenger Compartment: A Review of Current Practice, Journal of Sound and Vibrations, 80(2) (1982) 247-266.

[7] G. Sandberg, A New Strategy for Solving Fluid-Structure Problems, International Journal for Numerical Methods in Engineering, 38 (1995) 357-370.

[8] G. Sandberg, Acoustic and Interface Elements for Structure-Acoustic Analysis in CALFEM, Report TVSM-7113, Lund Institute of Technology, Division of Structural Mechanics, Lund (1996).

[9] G. Sandberg, P. Hansson, M. Gustavsson, Domain Decomposition in Acoustic and Structure-Acoustic Analysis, Accepted for publication in Computer Methods in Applied Mechanics and Engineering.

[10] G. Sandberg, Domain decomposition in structure-acoustic analysis, In S. N. Atluri, G. Yagawa, and T.A. Cruse, editors, Proc. of the International Conference on Computational Engineering Science '95 (1995) 857-862.

[11] Seock Hyun Kim, Jang Moo Lee, A Practical Method for Noise Reduction in a Vehicle Passenger Compartment, Journal of Vibration and Acoustics, 120 (1998) 199-205.

[12] S. Boily, F. Charron, The vibroacoustic response of a cylindrical shell structure with viscoelastic and poroelastic materials, Applied Acoustics, 58 (1999) 131-152.

[13] F. Fahy, Sound and Structural Vibration (Academic Press 1985).

[14] The MacNeal-Schwendler Corporation, MSC/NASTRAN ENCYCLOPEDIA - V70.5, (1998).

[15] K.-G. Olsson, P.-E. Austrell, M. Ristinmaa, G. Sandberg, CALFEM — a finite element toolbox to Matlab, Version 3.2, Report TVSM–9001, Lund Institute of Technology, Division of Structural Mechanics and Department of Solid Mechanics, Lund, Sweden (1999).

Paper 2

Reduction of structure-acoustic systems that include hysteretic damping

Peter Davidsson, Göran Sandberg
Division of Structural Mechanics
Lund Institute of Technology

Reduction of structure-acoustic systems that include hysteretic damping

Peter Davidsson, Göran Sandberg
Division of Structural Mechanics, Lund University, Sweden

Abstract

The structure-acoustic fluid problem is studied by use of the finite element method. In a previous paper the unsymmetrical system obtained by use of a pressure formulation for the fluid domain was reduced by use of the uncoupled modes of the structural and the fluid domain and was transformed into a symmetric standard eigenvalue problem. In the present paper the possibility of including hysteretic damping in this transformation, resulting in a complex-valued symmetric standard eigenvalue problem, is described. This provides a simple method for including damping in the frequency response analysis of structure-acoustic problems.

1 Introduction

In structure-acoustic finite element analysis the number of degrees of freedom can easily becomes very large. The element size needs to be small enough for the model to be able to describe the dynamic behavior of the system below the frequency limit of interest. In [1], [2] and [3] the size of the problem is reduced by substructuring of the coupled problem followed by modal reduction of it. The eigenmodes of the structural domain and of the fluid domain are calculated separately, the coupled system then being reduced by use of these uncoupled modes. After matrix scaling, the symmetric standard eigenvalue problem can be solved.
Damping is of considerable importance to the dynamic behavior of the system and needs to be accounted for in the analysis. The reduction of the coupled system is performed here by including hysteretic damping in both the structural and the fluid domain. This provides an averaged measure of the damping in each domain by use of two damping factors, η_s and η_f, both of them independent of frequency. The modal analysis of the damped coupled problem yields complex eigenvalues and eigenvectors. These modes can then be used in a modal frequency response analysis.

2 Substructuring and reduction

The damping is included at a constitutive level in the structural domain as a complex modulus of elasticity

$$\tilde{E}_s = (1 + i\eta_s)E_s \tag{1}$$

and in the fluid domain as a complex bulk modulus

$$\tilde{B}_f = (1 + i\eta_f)B_f \tag{2}$$

After finite element formulation has been performed the coupled structure-acoustic system can be described by an unsymmetrical equation system using a displacement formulation for the structural domain and a pressure formulation for the fluid domain. The damping that is introduced gives

$$\begin{bmatrix} \mathbf{M}_s & \mathbf{0} \\ \rho c^2 \mathbf{H}^T & \mathbf{M}_f \end{bmatrix} \begin{bmatrix} \ddot{\mathbf{d}} \\ \ddot{\mathbf{p}} \end{bmatrix} + \begin{bmatrix} \tilde{\mathbf{K}}_s & -\mathbf{H} \\ 0 & \tilde{\mathbf{K}}_f \end{bmatrix} \begin{bmatrix} \mathbf{d} \\ \mathbf{p} \end{bmatrix} = \begin{bmatrix} \mathbf{f}_b \\ \mathbf{f}_q \end{bmatrix} \tag{3}$$

where

$$\tilde{\mathbf{K}}_s = (1 + i\eta_s)\mathbf{K}_s; \qquad \tilde{\mathbf{K}}_f = (1 + i\eta_f)\mathbf{K}_f \tag{4}$$

which means an imaginary part due to damping being included in the structural and fluid stiffness matrices. The coupled system is reduced through use of uncoupled modes and the two domains are first analysed separately [1]. When hysteretic damping is included, this gives

$$\begin{aligned} \mathbf{\Phi}_s^T \mathbf{M}_s \mathbf{\Phi}_s &= \mathbf{I}_s & \mathbf{\Phi}_s^T \tilde{\mathbf{K}}_s \mathbf{\Phi}_s &= \tilde{\mathbf{D}}_s \\ \mathbf{\Phi}_f^T \mathbf{M}_f \mathbf{\Phi}_f &= \mathbf{I}_f & \mathbf{\Phi}_f^T \tilde{\mathbf{K}}_f \mathbf{\Phi}_f &= \tilde{\mathbf{D}}_f \end{aligned} \tag{5}$$

where the eigenvectors $\mathbf{\Phi}_s$ and $\mathbf{\Phi}_f$ are real and the eigenvalues of the two domains $diag(\tilde{\mathbf{D}}_s)$ and $diag(\tilde{\mathbf{D}}_f)$ are complex. Through matrix scaling of the reduced coupled problem, a symmetric system is obtained

$$\begin{bmatrix} \ddot{\zeta}_s \\ \ddot{\zeta}_f \end{bmatrix} + \begin{bmatrix} \tilde{\mathbf{D}}_s & -\sqrt{\rho c^2}\sqrt{\tilde{\mathbf{D}}_s}\mathbf{\Phi}_s^T \mathbf{H} \mathbf{\Phi}_f \\ -\sqrt{\rho c^2}\mathbf{\Phi}_f^T \mathbf{H}^T \mathbf{\Phi}_s \sqrt{\tilde{\mathbf{D}}_s} & \tilde{\mathbf{D}}_f + \rho c^2 \mathbf{\Phi}_f^T \mathbf{H}^T \mathbf{\Phi}_s \mathbf{\Phi}_s^T \mathbf{H} \mathbf{\Phi}_f \end{bmatrix} \begin{bmatrix} \zeta_s \\ \zeta_f \end{bmatrix} = \begin{bmatrix} \sqrt{\rho c^2}\sqrt{\tilde{\mathbf{D}}_s}\mathbf{\Phi}_s^T \mathbf{f}_b \\ \mathbf{\Phi}_f^T \mathbf{f}_q - \rho c^2 \mathbf{\Phi}_f^T \mathbf{H}^T \mathbf{\Phi}_s \mathbf{\Phi}_s^T \mathbf{f}_b \end{bmatrix}, \tag{6}$$

which allows the standard eigenvalue problem to be solved. This gives the eigenvalues and the right eigenvectors expressed in terms of the transformed coordinates $\mathbf{v}_R^\zeta$. In terms of the original coordinates the right eigenvectors become

$$\mathbf{v}_R = \begin{bmatrix} \mathbf{\Phi}_s & 0 \\ 0 & \mathbf{\Phi}_f \end{bmatrix} \begin{bmatrix} \left(\sqrt{\rho c^2}\sqrt{\tilde{\mathbf{D}}_s}\right)^{-1} & 0 \\ 0 & \mathbf{I}_f \end{bmatrix} \mathbf{v}_R^\zeta \tag{7}$$

For the left system, the coupled system matrices, $\mathbf{K}$ and $\mathbf{M}$, are transposed prior to reduction, i.e. $(\mathbf{v}_L^\zeta)^T\mathbf{K} = \lambda(\mathbf{v}_L^\zeta)^T\mathbf{M} \Leftrightarrow \mathbf{K}^T\mathbf{v}_L^\zeta = \lambda\mathbf{M}^T\mathbf{v}_L^\zeta$. The system matrices $\mathbf{M}_s$, $\tilde{\mathbf{K}}_s$, $\mathbf{M}_f$ and $\tilde{\mathbf{K}}_f$ are symmetric and the standard eigenvalue problem that yields the left eigenvectors can be written as

$$\begin{bmatrix} \tilde{\mathbf{D}}_s + \rho c^2 \mathbf{\Phi}_s^T \mathbf{H} \mathbf{\Phi}_f \mathbf{\Phi}_f^T \mathbf{H}^T \mathbf{\Phi}_s & -\sqrt{\rho c^2}\mathbf{\Phi}_s^T \mathbf{H} \mathbf{\Phi}_f \sqrt{\tilde{\mathbf{D}}_f} \\ -\sqrt{\rho c^2}\sqrt{\tilde{\mathbf{D}}_f}\mathbf{\Phi}_f^T \mathbf{H}^T \mathbf{\Phi}_s & \tilde{\mathbf{D}}_f \end{bmatrix} \begin{bmatrix} \zeta_s \\ \zeta_f \end{bmatrix} = \tilde{\lambda} \begin{bmatrix} \zeta_s \\ \zeta_f \end{bmatrix}. \tag{8}$$

In terms of the original coordinates the left eigenvectors become

$$\mathbf{v}_R = \begin{bmatrix} \mathbf{\Phi}_s & 0 \\ 0 & \mathbf{\Phi}_f \end{bmatrix} \begin{bmatrix} \mathbf{I}_s & 0 \\ 0 & \left(\sqrt{\rho c^2}\sqrt{\tilde{\mathbf{D}}_f}\right)^{-1} \end{bmatrix} \mathbf{v}_R^\zeta \tag{9}$$

3 Frequency response analysis

In order to use a modal description in the frequency response analysis the left and right eigenvectors of the coupled system are mass normalised,

$$\mathbf{v}_L^T \mathbf{M}_{sys} \mathbf{v}_R = \mathbf{I}_{sys} \qquad \mathbf{v}_L^T \mathbf{K}_{sys} \mathbf{v}_R = \mathbf{\Lambda} \tag{10}$$

where $\mathbf{I}_{sys}$ $(n \times n)$ is an identity matrix and $\mathbf{\Lambda}$ $(n \times n)$ contains the eigenvalues of the coupled system in the diagonal. n is the total number of structural and fluid eigenvectors used in reduction of the coupled system. Use of (7) and (9) in (10) gives

$$\left(\mathbf{v}_L^\zeta\right)^T \begin{bmatrix} \left(\sqrt{\rho c^2}\sqrt{\tilde{\mathbf{D}}_s}\right)^{-1} & \mathbf{0} \\ \sqrt{\tilde{\mathbf{D}}_s}^{-1} \mathbf{\Phi}_f^T \mathbf{H}^T \mathbf{\Phi}_s \sqrt{\tilde{\mathbf{D}}_f}^{-1} & \left(\sqrt{\rho c^2}\sqrt{\tilde{\mathbf{D}}_f}\right)^{-1} \end{bmatrix} \mathbf{v}_R^\zeta = \mathbf{I} \tag{11}$$

where $\mathbf{I}$ is an identity matrix. Calculating the reduced mass matrix $\hat{\mathbf{M}}$ inside the brackets in Eq. (11) allows the eigenvectors to be mass normalised,

$$(\mathbf{v}_L^\zeta)_i = \frac{(\mathbf{v}_L^\zeta)_i}{\sqrt{(\mathbf{v}_L^\zeta)_i \hat{\mathbf{M}} (\mathbf{v}_R^\zeta)_i}} \tag{12}$$

and

$$(\mathbf{v}_R^\zeta)_i = \frac{(\mathbf{v}_R^\zeta)_i}{\sqrt{(\mathbf{v}_L^\zeta)_i^T \hat{\mathbf{M}} (\mathbf{v}_R^\zeta)_i}} \tag{13}$$

The eigenvectors of the coupled problem can be mass normalised without of the mass matrix of the coupled system having to be set up. This allows the coupled system to be expressed in modal coordinates $\boldsymbol{\kappa}$,

$$\ddot{\boldsymbol{\kappa}} + \mathbf{\Lambda}\boldsymbol{\kappa} = \mathbf{v}_L^T \begin{bmatrix} \mathbf{f}_b \\ \mathbf{f}_q \end{bmatrix} \tag{14}$$

Modal frequency response analysis in which a harmonic force $F = \hat{F} \sin \bar{\omega} t$ is applied provides the system of uncoupled equations

$$(-\bar{\omega}^2 \mathbf{I} + \mathbf{\Lambda}) \hat{\boldsymbol{\kappa}} = \mathbf{v}_L^T \begin{bmatrix} \hat{\mathbf{f}}_b \\ \hat{\mathbf{f}}_q \end{bmatrix} \tag{15}$$

The frequency response can the be written in terms of original coordinates

$$\begin{bmatrix} \hat{\mathbf{d}} \\ \hat{\mathbf{p}} \end{bmatrix} = \mathbf{v}_R \hat{\boldsymbol{\kappa}} \tag{16}$$

4 Numerical example

The numerical part of the analysis was performed in Matlab using the finite element toolbox CALFEM [4]. An aluminium panel of 1.6 mm in thickness behind which a rectangular acoustic cavity is located has been analysed [5], see Fig. 1. The panel is 0.30 m long and 0.15 m wide. The air filled cavity is 0.15 m in depth. All the walls of the cavity except for the panel are rigid. The material data is given in Tab. 1. A normal incident pressure wave in the frequency range of 1-1000 Hz impinges on the outside of the panel. The sound transmission loss is measured between the outside and inside of the midpoint of the panel. The structural domain is described in use of 4-node quadrilateral plate elements derived in [6], and for the acoustic domain 8-node isoparametric elements with pressure formulation are used, see [2]. The analysis, which involves 910 degrees-of-freedom follows the steps described in the previous section. The sound transmission loss when the damping factors for the

Table 1: *Material data for the panel and cavity.*

Aluminum:	E	=	70	GPa
	ν	=	0.30	
	ρ	=	2700	kg/m^3
Air:	ρ	=	1.21	kg/m^3
	c	=	340	m/s.

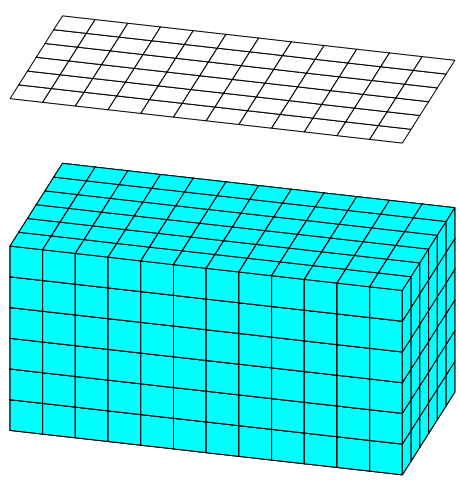

Figure 1: *A flexible panel backed with an acoustic cavity is studied.*

two domains are varied is plotted in Fig. 2. in Fig. 2.

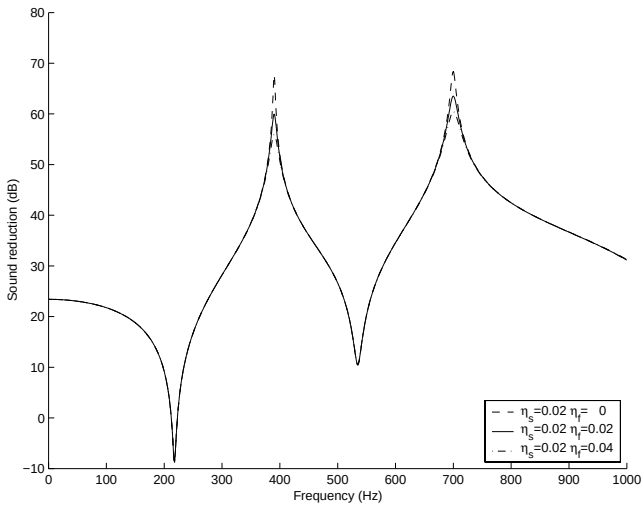

a)

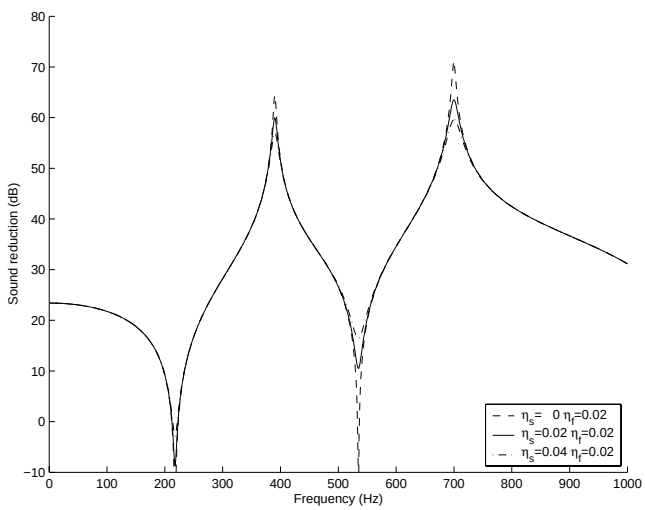

b)

Figure 2: *Sound transmission loss* $20^{10}log\frac{\hat{p}_0}{\hat{p}_{back}}$. *a) The damping in the fluid domain is varied, b) the damping in the structural domain is varied.*

5 Conclusions

The reduction of a structure-acoustic system presented earlier [1] is conducted here with inclusion of hysteretic damping in both the structural and the fluid domain. The reduction of the coupled problem can be performed as in the undamped case, except that the damping introduces complex arithmetics that yields imaginary parts for both the eigenvalues and the eigenvectors. Although the description of the damping this provides is very much simplified it is efficient from an engineering point of view since accurate estimates of damping are often difficult to obtain.

References

[1] G. Sandberg. A New Strategy for Solving Fluid-Structure Problems. International Journal for Numerical Methods in Engineering, vol 38, 357-370 (1995).

[2] G. Sandberg. Acoustic and Interface Elements for Structure-Acoustic Analysis in CALFEM. Report TVSM-7113, Lund Institute of Technology, Division of Structural Mechanics, Lund (1996).

[3] G. Sandberg, P. Hansson, M. Gustavsson. Domain Decomposition in Acoustic and Structure-Acoustic Analysis. Submitted for possible publication in Computer Methods in Applied Mechanics and Engineering.

[4] K.-G. Olsson, P.-E. Austrell, M. Ristinmaa, G. Sandberg. CALFEM — a finite element toolbox to Matlab, Version 3.2. Report TVSM–9001, Lund Institute of Technology, Division of Structural Mechanics and Department of Solid Mechanics, Lund, Sweden (1999).

[5] A.J. Pretlove, Forced vibrations of a rectangular panel backed by a closed rectangular cavity, Journal of Sound and Vibration, vol 3 (3), 252-261 (1966).

[6] J.-L. Batoz, M. B. Tahar, Evaluation of a new quadrilateral thin plate element, International Journal for Numerical Methods in Engineering, vol 18, 1655-1677 (1982).

Paper 3

Structure-acoustic analysis in an integrated modelling environment

Peter Davidsson, Göran Sandberg
Division of Structural Mechanics
Lund Institute of Technology

Gunnar Björkman, Johan Svenningstorp
Volvo Technological Development

Structure-acoustic analysis in an integrated modelling environment

Peter Davidsson, Göran Sandberg
Division of Structural Mechanics, Lund University, Sweden
Gunnar Björkman, Johan Svenningstorp
Volvo Technological Development, Göteborg, Sweden

Abstract

Structure-acoustic finite element analysis is implemented in an integrated modelling environment to demonstrate the possibilities such an environment provides. This allows research results to be used for analysing realistic vehicle structures, permitting research results and computational results to be readily displayed. Use of this environment aims at facilitating collaboration between different research projects and between researchers and industrial groups.

1 Introduction

The implementation of structure-acoustic finite element analysis in the Virtual Integral Vehicle Structure Laboratory (VIVS-lab) will be described. The VIVS-lab modelling environment aims at providing a common basis for communication between vehicle researchers and the vehicle industry, and at simplifying and facilitating cooperation and interaction between the two. In VIVS-lab, generic geometry models of different vehicle structures are created, allowing research results to be implemented and tested on realistic models. The present paper concerns the advantages of such an environment and the possibilities it opens up.
VIVS-lab is part of the Swedish national research programme IVS (Integral Vehicle Structure), which concerns future generations of vehicles. The programme aims at being multidisciplinary and at allowing different research projects to interact with each other. VIVS-lab was developed within the AML (Adaptive Modelling Language) modelling framework [6], aimed at facilitating the integration of the different parts of the product development cycle. AML is a modelling environment with an object-oriented architecture and with a graphical interface in which a parameterised

model of the product of interest can be studied. Integration of the development cycle is accomplished with the help of interfaces to a variety of other programs. The program to be used depends on the task, which may involve design (CAD) or finite element analysis (FEA), for example. The design process is divided up by the modelling environment into different objects, each representing a part of the total process. A given object can consist of several different subobjects.

2 Structure-acoustic analysis procedure

The finite element method can be used to study the interior noise level produced by structural vibrations. The structural domain and the fluid domain can be described by two separate equation systems of motion. For the structural domain

$$\mathbf{M}_s\ddot{\mathbf{d}} + \mathbf{K}_s\mathbf{d} = \mathbf{f}_b + \mathbf{H}\mathbf{p} \tag{1}$$

where $\mathbf{d}$ represent structural displacements and the dots indicate differentiation with respect to time. For the fluid domain

$$\mathbf{M}_f\ddot{\mathbf{p}} + \mathbf{K}_f\mathbf{p} = \mathbf{f}_q - \rho c^2\mathbf{H}^T\ddot{\mathbf{d}} \tag{2}$$

where $\mathbf{p}$ is the fluid pressure. For an account of the system matrices, see [1]. The coupling between the two domains is based on the force terms which include the coupling matrix $\mathbf{H}$ and allows the coupled system to be written as

$$\begin{bmatrix} \mathbf{M}_s & \mathbf{0} \\ \rho c^2\mathbf{H}^T & \mathbf{M}_f \end{bmatrix} \begin{bmatrix} \ddot{\mathbf{d}} \\ \ddot{\mathbf{p}} \end{bmatrix} + \begin{bmatrix} \mathbf{K}_s & -\mathbf{H} \\ 0 & \mathbf{K}_f \end{bmatrix} \begin{bmatrix} \mathbf{d} \\ \mathbf{p} \end{bmatrix} = \begin{bmatrix} \mathbf{f}_b \\ \mathbf{f}_q \end{bmatrix} \tag{3}$$

The strategy employed in the structure-acoustic analysis involves substructuring and modal reduction [1, 2]. First, the two eigenvalue problems, one for the structural domain and the other for the enclosed cavity domain, are solved separately. The uncoupled eigenmodes are then used to reduce the coupled problem by a change of base

$$\begin{bmatrix} \mathbf{d} \\ \mathbf{p} \end{bmatrix} = \begin{bmatrix} \Phi_s & \mathbf{0} \\ \mathbf{0} & \Phi_f \end{bmatrix} \boldsymbol{\xi} \tag{4}$$

Matrix transformation is used to derive two symmetric standard eigenvalue problems, providing the left and right eigenvectors needed to diagonalise the coupled equation system.

Determining the strength of the coupling between the modes of the two domains allows the most important uncoupled modes needed for describing the coupled system to be determined, see [4]. This is done by studying the modal coupling matrix

$$B_{ij} = \frac{\Phi_{si}^T\mathbf{H}\Phi_{fj}}{\omega_{sj}^2 - \omega_{ai}^2} \tag{5}$$

Those structural and fluid modes that generate values of considerable size in this coupling matrix are included in the reduction. It has been shown in [5] that hysteretic damping of the two domains can be included in this procedure. The damping is introduced in the structural domain at a constitutive level, as a complex modulus of elasticity

$$\tilde{E}_s = (1 + i\eta_s)E_s \tag{6}$$

and in the fluid domain as a complex bulk modulus

$$\tilde{B}_f = (1 + i\eta_f)B_f \tag{7}$$

This gives the coupled system complex eigenvalues and eigenvectors. It can then be reduced to a system of uncoupled equations expressed in terms of modal coordinates, $\boldsymbol{\zeta}$. Frequency response analysis using a harmonic force $F = \hat{F}\sin\bar{\omega}t$ is then applied to obtain the equation system

$$(-\bar{\omega}^2\mathbf{I} + \boldsymbol{\Lambda})\boldsymbol{\zeta} = \mathbf{v}_L^T \begin{bmatrix} \hat{\mathbf{f}}_b \\ \hat{\mathbf{f}}_q \end{bmatrix} \tag{8}$$

where $\boldsymbol{\Lambda}$ is an (n×n) matrix having the system eigenvalues in the diagonal, the left eigenvector being included in $\mathbf{v}_L$.

3 Implementation

Implementation of structure-acoustic analysis in AML and VIVS-lab will be described. Initially, a geometry object is created to serve as a simple model of a vehicle structure in which there is an interior cavity. This object is used to generate a finite element model, structure-acoustic analysis then being performed.
Various expressions employed in object oriented programming are needed. It is important here to distinguish between classes and objects. A defined class represents a description of a type of object, a given object being termed an instance of that class. A class typically contains three parts:

- inherit-from: States from which previously defined classes a new class inherits properties.
- properties: Defines the characteristics an object possesses.
- sub-objects: Objects of instantiated classes.

For example,

```
(define-class brick-class
  :inherit-from(box-class)
  :properties(
              color nil
              density nil
              )
 )
(define-class wall-class
  :inherit-from(object)
  :properties(
              wall-color red
              wall-density 720
              )
  :subobjects(
              (brick-1 :class 'brick-class
                       length 0.30
                       width  (/ (the length) 2)
                       color  (the superior superior wall-color)
                       density ^^wall-density)
              )
 )
```

A `brick-class` is created here, this is in turn being used to create a wall. This class inherits from the `box-class` those properties needed to describe a brick, except

for color and density, which are added in creating the class. The `wall-class` is then created, using bricks instantiated from the `brick-class`. `nil` states that the property has not yet been defined. `the` is used to find properties or sub-objects of an object. By use of the `superior` statement, search for a property or subobject one level above the current one is carried out. In the `wall-class`, the `color` property of `brick-1` is determined, obtained from the `wall-color` two levels higher up. The `density` property is likewise determined from two levels higher up using the shortcut character `^`.
The `acoustic-model-class` is created in the AML environment for the analysis here, three sub-objects being instantiated so as to permit the analysis to be performed. The AML-code for the object in question is,

```
(define-class acoustic-model-class
  :inherit-from(object)
  :properties(
              )
  :subobjects(
            (acoustic-cavity :class 'acoustic-cavity-class
               )
            (acoustic-model-mesh :class 'acoustic-model-mesh-class
               )
            (acoustic-analysis :class 'acoustic-analysis-class
               )
             )
 )
```

Each of these sub-objects is described in detail below, interesting aspects of the AML-code also being shown.

3.1 Geometry

A parameterised geometry model is created. In Fig. 1, the geometry object has been instantiated in the graphical interface, where the editable properties can be modified. Properties are made editable in the graphical interface by their being defined as an `editable-data-property-class`, as can be seen in the AML-code below for the property of length . On the basis of such properties, design points can be created from which curves can be derived. The curves are used then to generate surfaces. In AML-code, the geometry model is written as:

```
(define-class acoustic-cavity-class
  :inherit-from (object)
  :properties(
          property-objects-list (list
                                    (the superior length self))
          (length :class 'editable-data-property-class
                  label "Cavity length"
                  formula (default 1.8))
...
              )
  :subobjects(
     (front-coordinate-system :class 'coordinate-system-class
            origin (list ^^front-down 0 0)
            display? 'nil)
...
     (point-1 :class 'point-object
            coordinates (list 0 0 0)
            reference-coordinate-system ^^front-coordinate-system)
...
     (curve-1 :class 'curve-from-points-class
            points-coordinates-list (list
                                       (center-of-object ^point-1)
                                       (center-of-object ^point-17)
                                       (center-of-object ^point-2)))
...
     (panel-1 :class 'skin-surface-from-curves-grid-object
            ucurve-objects (list ^curve-1 ^curve-3)
            vcurve-objects (list ^curve-2 ^curve-17 ^curve-4))
               )
 )
```

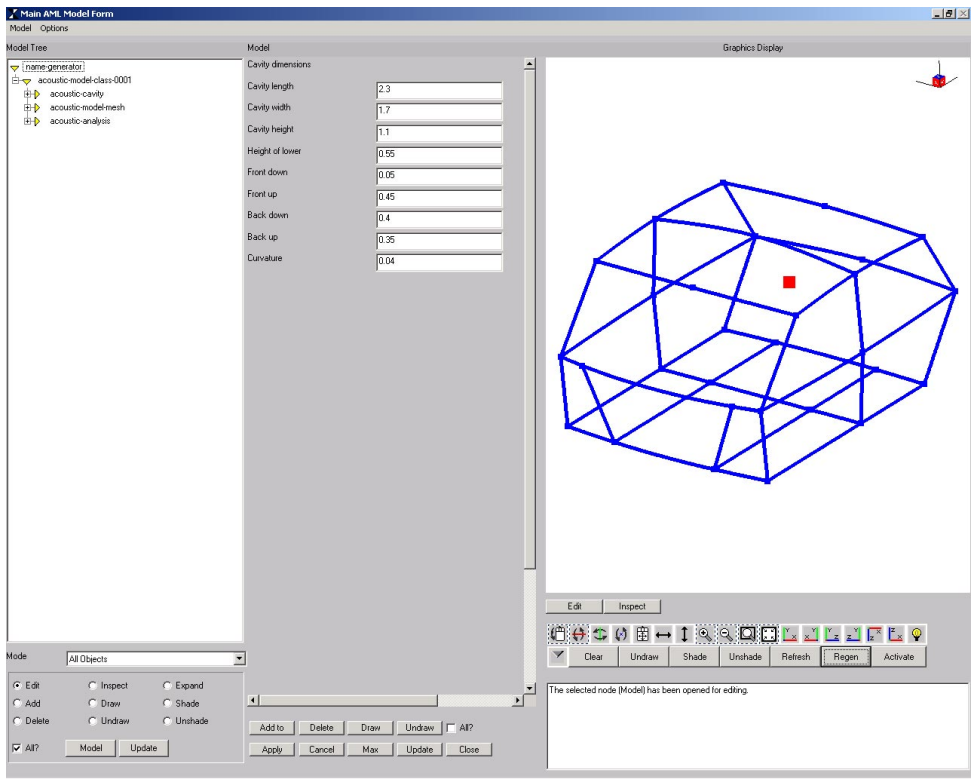

Figure 1: *The AML graphical interface in which the geometry model has been plotted in the graphics display window. The object tree to the left shows the objects that have been instantiated. The editable properties of a given object can be seen near the middle part of the interface. In the acoustic cavity, the length, width, height, etc. can be modified.*

3.2 Meshing

From the geometry objects a mesh is generated. The objects need to contain all the information necessary to perform the operations called for, such as the minimum element size, for example. This is accomplished by tagging the geometry objects, giving them the attributes needed to generate the mesh.
The geometry objects created, such as points, curves and surfaces, need to be joined together to form a single object in order to be meshed. The surface thus created, which encloses the cavity is used to generate a solid object having this surface as its boundary.
An object in which the solid geometry is meshed by use of the AML-interface to MSC/Patran is generated. This object can then be queried to determine the finite elements of the different regions. An object tree showing the process just described is shown in Fig. 2. The solid geometry object and the meshes derived from it are plotted in Fig. 3. The coupling elements between the structural domain and the fluid domain used for determining the coupling matrix **H** contain information about which nodes from the two domains coincide. The mesh object generates a (coinciding) mesh of shared nodes from the two domains at the boundary between them. The shell elements in contact with the fluid can thus also be used as coupling elements, having all the information needed.

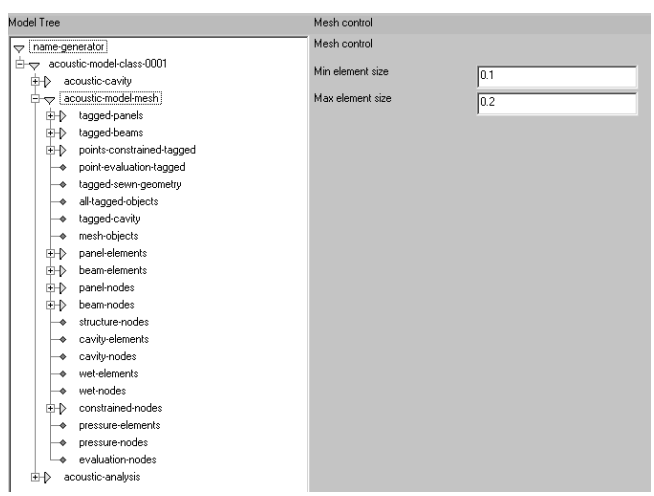

Figure 2: *An object tree showing the steps of tagging the surfaces and curves and then joining the geometry objects to one solid object. This is then meshed, allowing the finite elements generated in each domain to be queried. The element size can also be edited.*

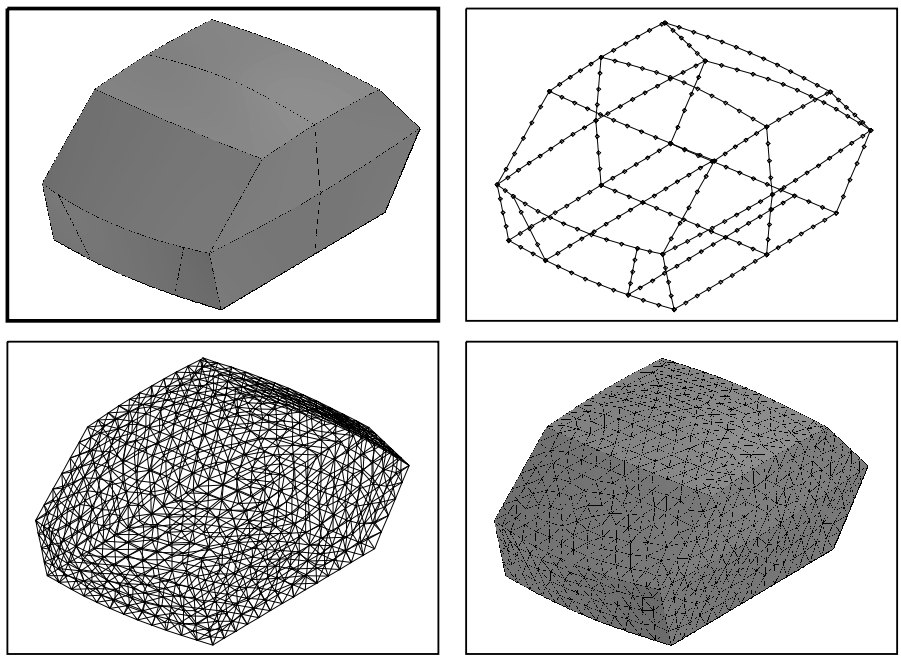

Figure 3: *a) The solid geometry object. b) The beam elements of the structural domain. c) The shell elements of the structural domain. d) The solid elements of the acoustic fluid domain.*

3.3 Structure-acoustic analysis

The structure-acoustic analysis involves three different parts. The structural and the fluid domain are analysed separately, a coupled analysis then being performed. An analysis class is created in which the properties written in the AML-code below define the finite elements and nodes describing the analysis model employed. There are also editable properties which control the analysis. These can be seen in Fig. 4, in which the object tree for the analysis is shown. The AML-code for this object is

```
(define-class acoustic-analysis-class
   :inherit-from(object)
   :properties (
               ...
               mesh-object                nil
               beam-mesh-query            nil
```

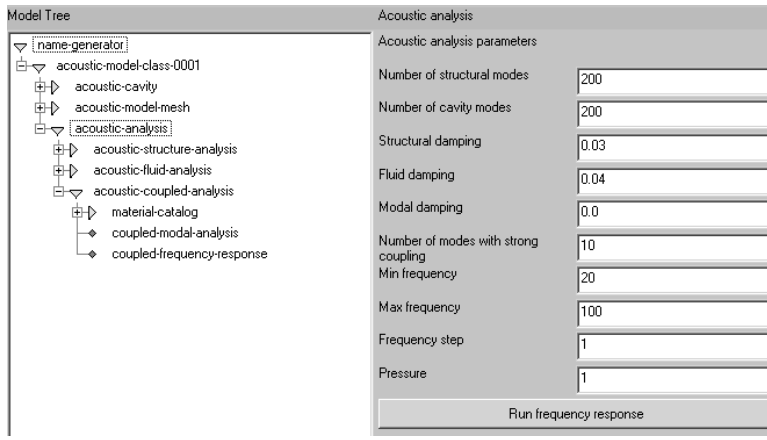

Figure 4: *The object tree and the editable data for structure-acoustic analysis.*

```
                panel-mesh-query            nil
                structure-node-query        nil
                constraint-nodes-query      nil
                cavity-mesh-query           nil
                cavity-node-query           nil
                wet-element-mesh-query      nil
                wet-node-mesh-query         nil
                force-node-mesh-query       nil
                evaluation-node-mesh-query  nil
                number-nodes-structure      nil
                number-nodes-cavity         nil
                material-list-cavity        nil
                nastran-file-structure      nil
                nastran-file-cavity         nil
                )
  :subobjects(
          (acoustic-structure-analysis
                  :class 'acoustic-structure-analysis-class)
          (acoustic-fluid-analysis
                  :class 'acoustic-fluid-analysis-class)
          (acoustic-coupled-analysis
                  :class 'acoustic-coupled-analysis-class)
              )
)
```

Uncoupled modal analysis

Two classes are created for performing the uncoupled modal analysis by use of MSC/Nastran [7], one of them for the structural domain and the other for the fluid domain. For each class, a list of properties defines the materials, finite elements, boundary conditions and analysis parameters of the domain in question. The AML interface to MSC/Nastran is instantiated so as to determine the uncoupled eigenmodes of the two domains. For the structural domain the AML-code becomes

```
(define-class acoustic-structure-analysis-class
   :inherit-from(analysis-model-class)
   :properties (
                analysis-type               :modal
                element-set-1d-objects-list nil
                element-set-2d-objects-list nil
                node-set-objects-list       nil
                property-set-objects-list   nil
                load-case-objects-list      nil
                material-catalog-object     nil
                material-catalog-file-name  nil
                materials-list              nil
                eigenvalue-data-object      nil
                mesh-object                 nil
                )

   :subobjects (
...
          (nastran-analysis-structure :class 'nastran-analysis-class
                  analysis-model-object  (the superior superior)
                  nastran-file-name "acoustic-structure.bdf")
                )
 )
```

Coupled analysis

The coupled analysis performed in Matlab [8] consists of two parts. Modal analysis is first used to determine the eigenvalues and the left and right eigenvectors. These results are used then, in the second step, for determining the frequency response to a given excitation. Two classes with an interface to Matlab perform the analysis. These are instantiated as subobjects in the class that performs the coupled analysis, see the object tree in Fig. 4. The properties needed for the analysis is given in the `acoustic-analysis-class` defined previously. The class performing the modal analysis has the following properties:

- matlab-file-name: Name of the matlab m-file created for the analysis.
- analysis-directory: Directory in which the analysis is performed.
- matlab-file-path: Name of the matlab m-file, together with the entire path required for finding it.
- analysis-model-object: Contains the description of the model and those parameters needed to perform the analysis.
- data-file: Generates a m-file with the needed data for performing the analysis by means of the `export-matlab-modal-analysis-file` method.
- analysis-results-file: Name of the mat-file where the results are saved.
- run-analysis: Executes the created m-file in Matlab.

This is written in AML-code as

```
(define-class structure-acoustic-modal-analysis-class
   :inherit-from(object)
   :properties(
     matlab-file-name
           (default (format nil "~a~a" "modal_analysis" ".m"))
     analysis-directory
           (logical-path :matlab-data
           (write-to-string (object-name (the superior))))
     matlab-file-path
           (and (or (probe-file ^analysis-directory)
                 (create-directory ^analysis-directory))
                 (logical-path ^analysis-directory ^matlab-file-name))
     analysis-model-object
            nil
     data-file
            (export-matlab-modal-analysis-file
                 (the superior)
                 ^analysis-model-object
                 ^matlab-file-path)
     analysis-result
            (format nil "~a~a"
                    (drop-dot-extension ^matlab-file-path) ".mat")
     run-analysis
            (progn
                 ^data-file
                 (cd ^analysis-directory)
```

```
                    (run-program
                        (format nil "~a ~a"
                        "matlab /minimize /r"
                        (drop-dot-extension ^matlab-file-name)))
                    ^analysis-result)
                   )
    )
```

Frequency response analysis has the same structure but has an extra property that has been added, one which points to the results file that the modal analysis has generated.

3.4 Results

Structure-acoustic finite element analysis can be performed in an automated fashion for determining, at the evaluation nodes in the cavity, the sound level due to a force that is applied to the structure. The geometry model is parameterised and a mesh is generated with an interface to MSC/Patran allowing the finite elements and nodes for each domain to be derived. The uncoupled eigenvalue analysis is performed in MSC/Nastran, two modes from each domain are plotted in Figs. 5 and 6. These uncoupled modes are then used in the coupled analysis. Modal analysis is performed first followed by frequency response analysis. The sound level at the driver's ear which is due to a uniform pressure in the frequency range from 20 to 100 Hz being applied to the outside of the front wall is shown in Fig. 7.

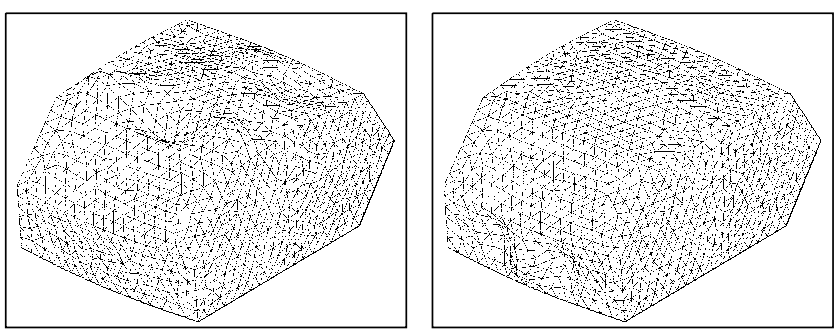

Figure 5: *Uncoupled structural modes.*

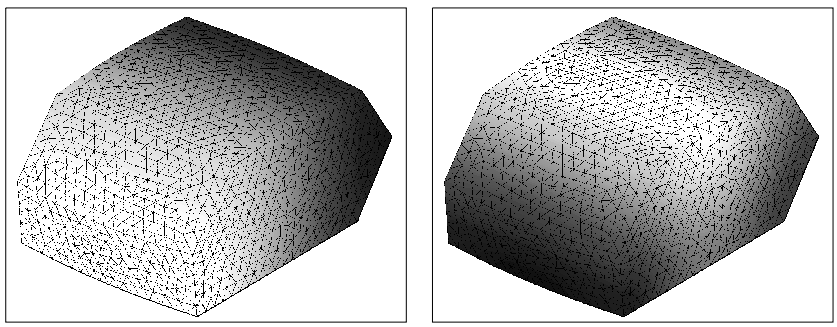

Figure 6: *Uncoupled fluid modes.*

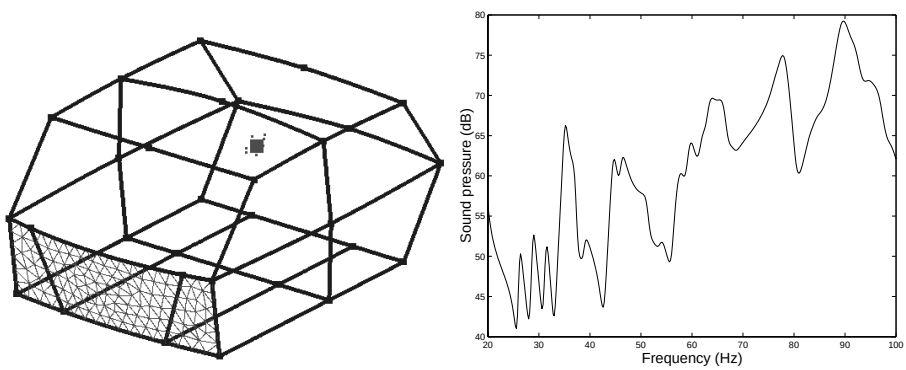

a) b)

Figure 7: *a) The finite elements located where the pressure is applied and the evaluation nodes at the driver's ear. b) The sound pressure level at the drivers ear when a uniform pressure of 1 Pa is applied. The analysis parameters employed can be seen in Fig. 4.*

4 Future work - Truck cabin

The next step is to apply the structure-acoustic analysis class to a more complex structure. This is to be done on a truck cabin generated in the VIVS-lab environment, see Fig. 8.

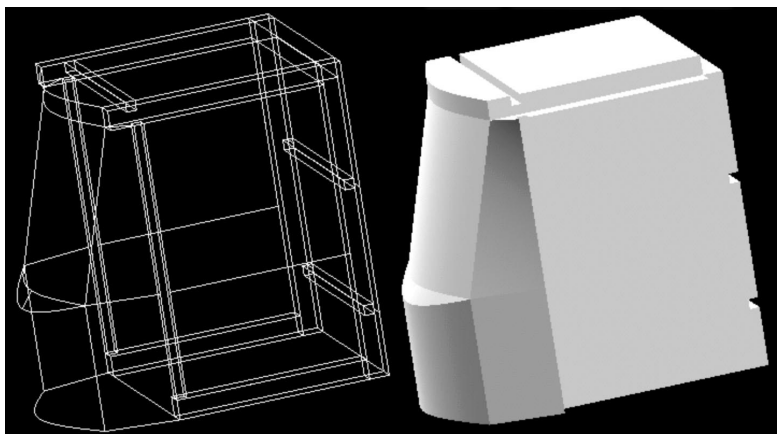

Figure 8: *A truck cabin is generated in VIVS-lab. The geometry model of the structural and the cavity domain are displayed.*

5 Conclusions

Using the model environment described enables an analysis to be performed in which different programs are used in an integrated fashion. For each task to be performed, the most effective program can be employed. This model environment also provides a common basis for collaboration between research projects and facilitates communication between researchers and industrial groups.

References

[1] G. Sandberg, A New Strategy for Solving Fluid-Structure Problems, International Journal for Numerical Methods in Engineering, vol 38, 357-370 (1995).

[2] G. Sandberg, Acoustic and Interface Elements for Structure-Acoustic Analysis in CALFEM, Report TVSM-7113, Lund Institute of Technology, Division of Structural Mechanics, Lund (1996).

[3] K.-G. Olsson, P.-E. Austrell, M. Ristinmaa, G. Sandberg, CALFEM — a finite element toolbox to Matlab, Version 3.2, Report TVSM–9001, Lund Institute of Technology, Division of Structural Mechanics and Department of Solid Mechanics, Lund, Sweden (1999).

[4] G. Sandberg, P. Davidsson, Choosing modes in the reduction of structure-acoustic systems, Submitted to Computer Methods in Applied Mechanics and Engineering (2001).

[5] P. Davidsson, G. Sandberg, Reduction of structure-acoustic systems that include hysteretic damping, Submitted to Computer Methods in Applied Mechanics and Engineering (2001).

[6] Technosoft Inc., AML Version 3.2.0, Reference manual, (2001).

[7] The MacNeal-Schwendler Corporation, MSC/NASTRAN ENCYCLOPEDIA - V70.5, (1998).

[8] The Mathworks Inc., Matlab Reference Guide, (2000).

Paper 4

Analysis of double-leaf walls within the low frequency range using the finite element method

Peter Davidsson, Per-Anders Wernberg, Göran Sandberg
Division of Structural Mechanics
Lund Institute of Technology

Analysis of double-leaf walls within the low frequency range using the finite element method*

Peter Davidsson, Per-Anders Wernberg, Göran Sandberg
Division of Structural Mechanics, Lund University, Sweden

Abstract

Double-leaf walls consisting of sheet-metal wall studs covered by plaster boards were studied be means of structure-acoustic finite element analysis to determine the sound reduction within the low frequency range of a wall, emphasis being placed on the effects of the wall stud design. A parametric study was also performed to investigate the influence on the sound reduction of different properties of the wall, including the thickness of the wall, the number of plaster boards employed, the stiffness of the wall stud web and the boundary conditions. The influence on the sound transmission of the room dimensions is also studied.

1 Introduction

Walls constructed of sheet-metal studs to which sheeting material is attached have become very popular in housing construction. Their light weight and the efficient building process that use of them facilitates are some of the advantages. One problem, however, is the low degree of sound reduction they provide at low frequencies as compared with that provided by a heavier wall. The Swedish building code regulates sound transmission down to 50 Hz and the reduction in sound transmission a wall achieves being determined by placing it in between two rooms, the one a sending room with a loudspeaker and the other a receiving room. The sound level in each of the two rooms are measured indicating the sound reduction the wall provides [1, 2]. The present study aims at predicting the sound reduction of such a wall on the basis of the properties of the wall studs. These properties can be determined by a detailed finite element analysis of the cross section, making it possible to predict the sound reduction the wall achieves on the basis of a drawing of the stud profile.

*This work has been conducted in close cooperation with Hans Larsson at Lindab Profil AB

The design process involved is exemplified by analysis of a standard wall stud and a newly designed wall stud.
The method of measuring sound transmission is based on the assumption of the sound fields being diffuse, which is not the case in the low frequency range. There, the modal density is low and transmission is strongly affected by the separate structural modes and by the separate acoustic modes in the two rooms. It is thus of interest to investigate the behavior of the coupled sending room-wall-receiving room system to determine the influence of various structural properties on the sound transmission. To this end, a parametric study employing the finite element method and involving the following parameters was carried out:

- The thickness of wall
- Stiffness of the wall studs
- Number of plaster boards
- Boundary conditions.

Calculations were performed for the two wall stud distances of 0.45 m and 0.60 m. The effect of the room dimensions on the sound transmission was also studied, a matter investigated earlier in [6]. The finite element model employed is based on the setup in which the measurements are performed. To be able to interpret measurement results obtained and suggest improvements in design of the wall studs it is important to understand the dynamic behavior of the wall and the influence of the different parts of the wall in question.

2 Structure-acoustic finite element analysis

The finite element model is based on the setup used for the measurements, see Fig. 1, in which the dimensions are given. The finite element model is shown in Fig. 2, the height and width of the rooms being regarded as equal to the dimensions of the wall separating them. The depths (in the direction normal to the wall that is studied) both for the sending room and the receiving room in the calculation are equal to the depths for the rooms in the measurement.

2.1 Analysis procedure

Finite element formulations for both the structural domain (the wall) and the fluid domains (in each of the two rooms and in the wall cavities) provides the equation of motions for the structural domain

$$\mathbf{M}_s\ddot{\mathbf{d}} + \mathbf{K}_s\mathbf{d} = \mathbf{f}_b + \mathbf{H}\mathbf{p} \tag{1}$$

and for fluid domain i

$$\mathbf{M}_f^i \ddot{\mathbf{p}}^i + \mathbf{K}_f^i \mathbf{p}^i = \mathbf{f}_q^i - \rho c^2 \mathbf{H}^{i\,T} \ddot{\mathbf{d}} \tag{2}$$

For an account of the system matrices see [3]. The matrix $\mathbf{H}^i$ pertains to the coupling between the structural domain and fluid domain i. The matrix which couples the structural domain with each of the fluid domains is $\mathbf{H} = [\mathbf{H}^1 ... \mathbf{H}^i ... \mathbf{H}^M]$, where M is the number of fluid domains involved. This yields the coupled problem

$$\begin{bmatrix} \mathbf{M}_s & \mathbf{0} \\ \rho c^2 \mathbf{H}^T & \mathbf{M}_f \end{bmatrix} \begin{bmatrix} \ddot{\mathbf{d}} \\ \ddot{\mathbf{p}} \end{bmatrix} + \begin{bmatrix} \mathbf{K}_s & -\mathbf{H} \\ 0 & \mathbf{K}_f \end{bmatrix} \begin{bmatrix} \mathbf{d} \\ \mathbf{p} \end{bmatrix} = \begin{bmatrix} \mathbf{f}_b \\ \mathbf{f}_q \end{bmatrix} \tag{3}$$

The analysis involves first solving the eigenvalue problems for the uncoupled structural domain and for the fluid domains separately. The coupled system is then reduced using the uncoupled modes by the change of base

$$\begin{bmatrix} \mathbf{d} \\ \mathbf{p} \end{bmatrix} = \begin{bmatrix} \Phi_s & \mathbf{0} \\ \mathbf{0} & \Phi_f \end{bmatrix} \boldsymbol{\xi} \tag{4}$$

where $\Phi_f = diag([\Phi_f^1 ... \Phi_f^i ... \Phi_f^M])$. The coupled unsymmetrical eigenvalue problem is made symmetric by use of a matrix transformation, see [3]. The sound levels in

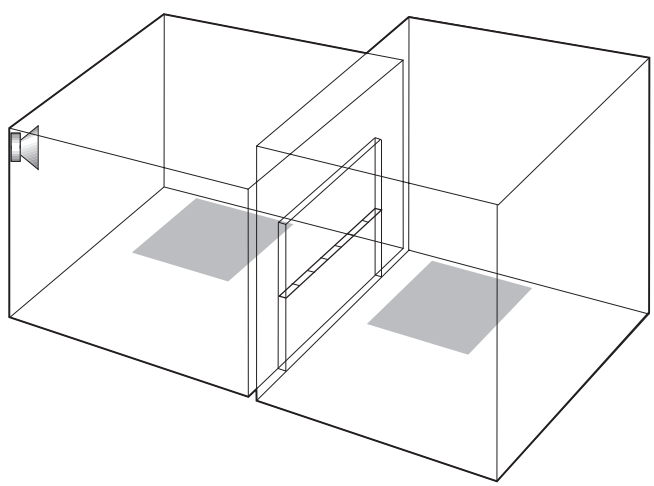

Figure 1: *Measurement setup. The opening in the wall is 4.2 m long and 2.59 m high. The dimensions of the sending room are: depth=4.91 m, width=6.15 m (parallel to the studied wall) and height=3.56 m. The dimensions of the receiving room are depth=4.91 m, width=6.15 m (parallel to the wall being studied) and height=4.26 m.*

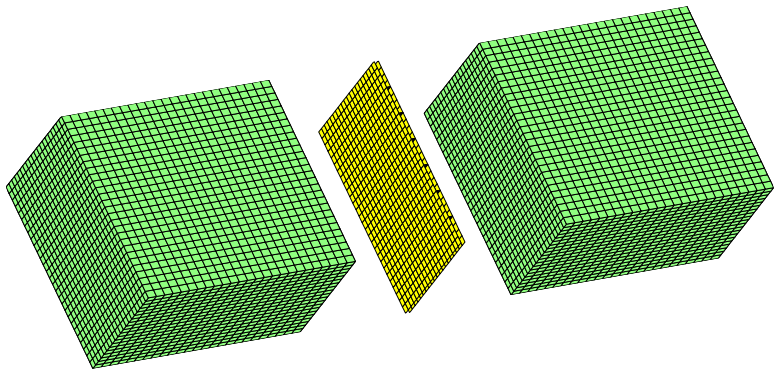

Figure 2: *Finite element model*

the two rooms are determined by means of modal frequency response analysis. A loudspeaker is placed at the position indicated in Fig. 1 and at two additional points in the sending room. The sound levels are measured then at the nodes located in the central portion of the two cavities, which is the shaded area in Fig. 1. The Reduction index, R, is determined by

$$R = L_s - L_r - 10\log(\frac{A}{S}) \tag{5}$$

where L_s is the spatial average of the sound levels in the sending room as calculated at N nodes with sound pressure L_{pn},

$$L_s = \sum_{n=1}^{N} 10\log(\frac{1}{N}10^{L_{pn}/10}) \tag{6}$$

and L_r is the spatial average of the sound levels in the receiving room. S is the area of the wall being studied and A is the absorption area in the receiving room, which can be expressed in terms of the reverberation time T, and the volume of the room V,

$$A = 0.16\frac{V}{T} \tag{7}$$

The loss factor $\eta = 0.02$, which is independent of frequency, is used in the analysis. The reverberation time then is

$$T = \frac{2.2}{f\eta} \tag{8}$$

where f is the frequency. Eq. 5 then becomes

$$R = L_s - L_r - 10\log(\frac{A}{S}) = L_s - L_r - 10\log(0.073D_{zr}f\eta) \tag{9}$$

D_{zr} is the depth of the receiving room perpendicular to the wall being studied. Frequency response analysis is carried out for the interval 22 Hz to 178 Hz with a frequency step of 1 Hz between successive evaluations.

2.2 Finite element model

The structure consists of sheet-metal wall studs on both sides of which plaster boards are attached with screws. The material properties are listed in Tab. 1. The plaster boards, which are 12.5 mm thick, are modelled by use of shell elements. It is assumed that when one board is placed on top of another there is no friction between the plates, there being a doubling of the moment of inertia as compared with a single plate. The wall studs, which are 0.5 mm thick, are modelled using shell elements for the web, and beam elements for the flanges. The screws connecting the plaster boards to the wall studs are placed with a distance of 0.2 m between adjacent screws, modelled as springs connecting the nodes at the wall stud-plaster board interface. Measurements were performed to determine the stiffness of the in-plane deformation. The coupling to the plaster boards in the normal direction and the rotational coupling in all three directions are assumed to be rigid. The wall cavities are regarded as being empty, i.e. as containing no absorption material. The material properties of the air can be found in Tab. 1.

Table 1: *Material data.*

Wall studs:				
	E	=	210	GPa
	ν	=	0.30	
	ρ	=	7800	kg/m^3
Plaster boards:				
	E	=	2.5	GPa
	ν	=	0.30	
	ρ	=	720	kg/m^3
Fasteners:				
	K	=	500	kN/m
Air:				
	ρ	=	1.21	kg/m^3
	c	=	340	m/s.

3 Analysis of wall design

The study aims to predict the change in sound reduction by the wall which a particular change in the wall stud design would produce. The properties of a wall stud are determined on a basis of a detailed finite element analysis. These properties are then transformed into a simplified model of the wall stud used in the coupled structure-acoustic calculations. The analysis is carried out for both a standard, type 1 wall stud, and a new, or type 2 wall stud, the results for the two being compared.

3.1 Static stiffness of wall stud

Static analysis was performed to determine the difference in bending stiffness of the two different wall studs. The wall studs analysed were 95 mm in height. The stiffness when the two flanges were displaced in the manner shown in Fig. 3 was calculated and was measured. To calculate the static stiffness, a detailed finite element model of the type 2 wall stud, as shown in Fig. 4, was created. The perforation was modelled so as to resemble the actual structure. A similar mesh without perforation was used for modelling the standard wall stud. The sheet metal was 0.5 mm thick, the material data being presented in Tab. 1. A prescribed displacement of 0.01 m was applied to one of the flanges to produce a constraint force, allowing the stiffness to be calculated. The results for a 0.195 m stud piece are presented in Tab. 2. The stiffness of the wall studs was also measured, wall stud pieces 0.195 m in length being studied. Each piece was clamped at both flanges, one of the supports being displaced giving force-displacement curves shown in Fig. 4 b). The stiffness was determined by linear regression, giving the results shown in Tab. 2 in which the calculated values for a wall stud piece of the same length are also presented. The calculated and the measured values agree well, both studies showing that the new

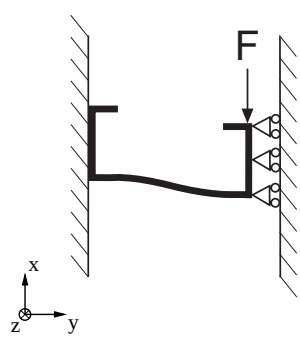

Figure 3: *Deformation shape used in calculations and measurements.*

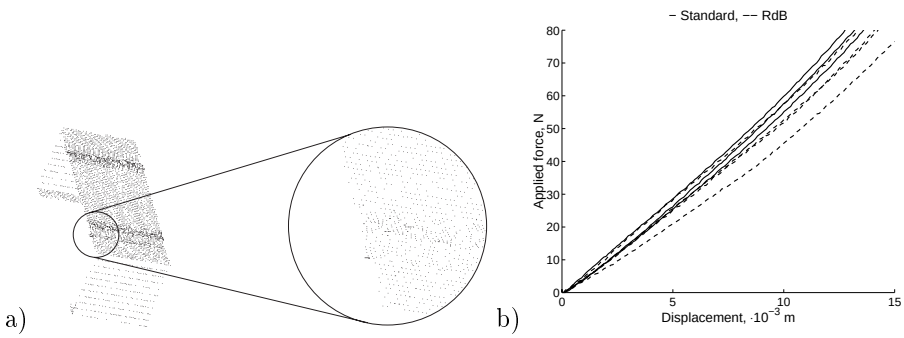

Figure 4: *a) Finite element model of a wall stud. b) Measured stiffness of the deformation shape that was studied.*

wall stud is weaker then the standard one. The wall stud properties can be derived from a finite element model based on a drawing. These properties are then used in the structural-acoustic calculations in the next section.

3.2 Static stiffness of fastening

The stiffness of the fastening between the sheet-metal wall studs and the plaster boards was also studied, using the setup shown in Fig. 5 a) used in [7] for wooden wall studs. The material thickness of the wall studs that were studied was 0.5 mm and 0.7 mm, respectively, the stiffness of the juncture to a single plaster board 12.5 mm in thickness or two of them placed on top of each other, being tested. The force-deformation curves that were measured for both thicknesses of the sheet-metal in the wall stud and for a single plaster board are shown in Fig. 5 b). The stiffness for the case with a single plaster board was found to be to 0.5 kN/m, see [8]. For the double plaster boards this same value was used in the structure-acoustic calculations presented in the next section.

Wall studs	Measured	FEM
Standard	6.1	6.06
RdB	5.7	5.53
Difference (%)	6.3	8.8

Table 2: *Measured and calculated stiffness.*

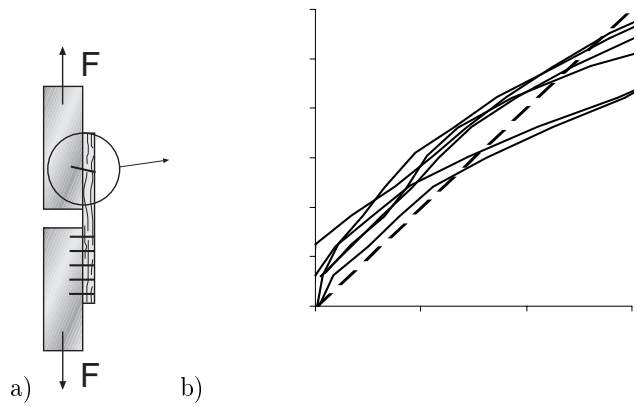

Figure 5: *a) Experimental setup to determine the in-plane stiffness of the fasteners. b) Force-displacement curve for single plaster board and sheet metal thickness 0.5 mm and 0.65 mm for the wall stud. The solid lines are results from measurements and the dotted line the stiffness value used in the structure-acoustic calculations in the next section.*

3.3 Structure-acoustic calculations

The sound reduction achieved by the wall was calculated with use of the standard wall studs 0.070 m in height, with a double layer of plaster boards on each side. The distance between adjacent wall studs was either 0.45 or 0.60 m, see Fig. 6, in which the calculated results, involving both the frequency response curve and the results in third octave bands, are compared with the measured ones. Despite the simplifications made, the measurements and the calculations of the sound reduction the walls achieve agree well. The decrease in stiffness of the type 2 wall studs has no effect on the sound transmission. In the next section the results of a parametric study to determine the contribution of the various parameters to the sound reduction of the wall are reported.

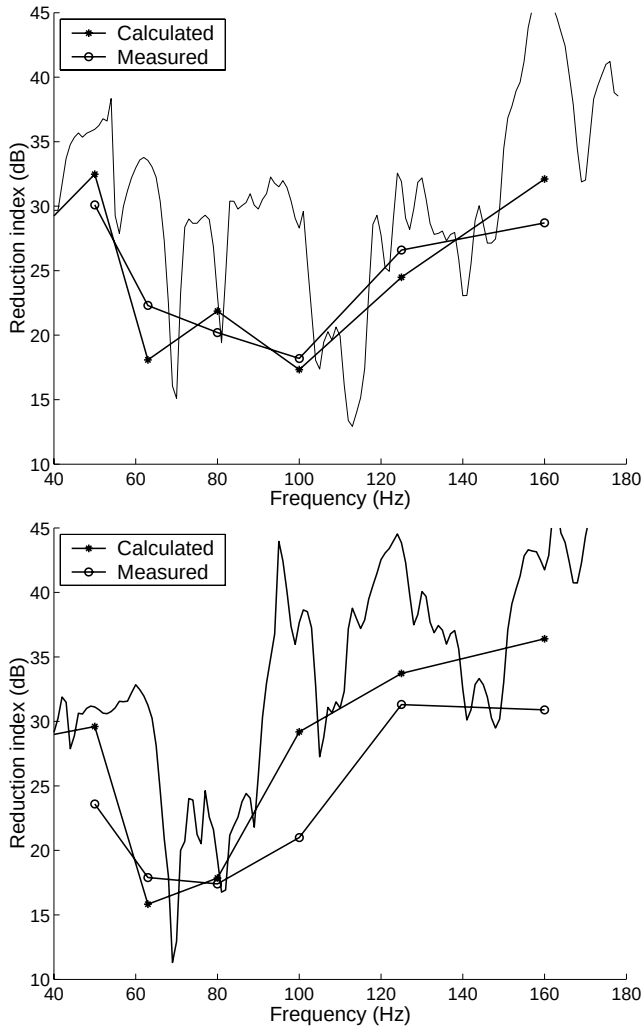

Figure 6: *Computed and measured reduction in sound. The wall stud is 0.070 m in height. a) Distance between the wall studs of 0.45 m. b) Distance between the wall studs of 0.60 m.*

4 Parametric study

Coupled structure-acoustic finite element analysis was performed to determine the influence of the different parts of the wall. The previously defined parameters were varied as follows:

- The thickness of the wall, $t_w = 0.070$, 0.095 or 0.120 m.
- Distance between the wall studs, $s = 0.45$ or 0.60 m.
- Number of plaster boards, $n_p = 1$ or 2.
- Bending stiffness of the stud web, $I_web = t_{web}^3/12$ or $t_{web}^3/24$.
- Boundary condition of the wall: free or clamped.
- Depth of the receiving room, $D_r = 4$, 4.92 or 5 m.

The sound reduction of the different walls was evaluated. The results are displayed both for the frequency step used in the calculations and for the third octave bands. In each section the results obtained in using distances of 0.45 m and 0.60 m, respectively, between the wall studs are shown. When not stated otherwise wall is 0.095 m thick with double plaster boards on each side.
As expected, an increase in the thickness of the wall and in the number of plaster boards employed results in an increase in the sound reduction, see Figs. 7 and 8. At certain frequencies, however, the sound reduction can be lower when the wall thickness is higher. When the bending stiffness of the wall stud web is reduced to be only half as great the sound reduction of the wall is nevertheless virtually unaffected, see Fig. 9. At low frequencies the wall stud can influence the sound transmission by changing the global bending stiffness of the wall stud which would either lead to the undesired effect of decreasing the static stiffness of the wall or, in the case of the stiffer wall studs, of increasing the sound transmission at higher frequencies. Changing the boundary conditions of the wall from hinged to clamped has only a slight effect on the sound transmission, see Fig. 10. In contrast, the dimensions of the room have a strong effect on the results, see Fig. 11. Reducing the depth of the receiving room to 4 m increases the sound reduction occurring in the third octave band at 60 Hz by nearly 15 dB. Even small changes here affect the results. A 9 cm increase of the depth of the room results in a 2-3 dB increase in the sound reduction in each third octave band within the region of 63 to 100 Hz. The sending room and the receiving room should not be of the same dimensions since, when the modes of the two rooms are matching the sound transmission increases.
As can be seen, there are some frequencies at which the sound reduction obtained is very low for each of the configurations. The behavior of the room-wall-room system at one of these frequencies is examined in the next section.

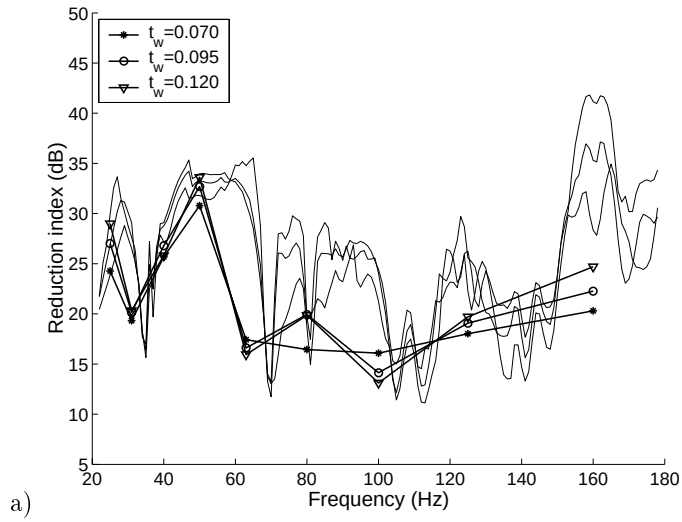

a)

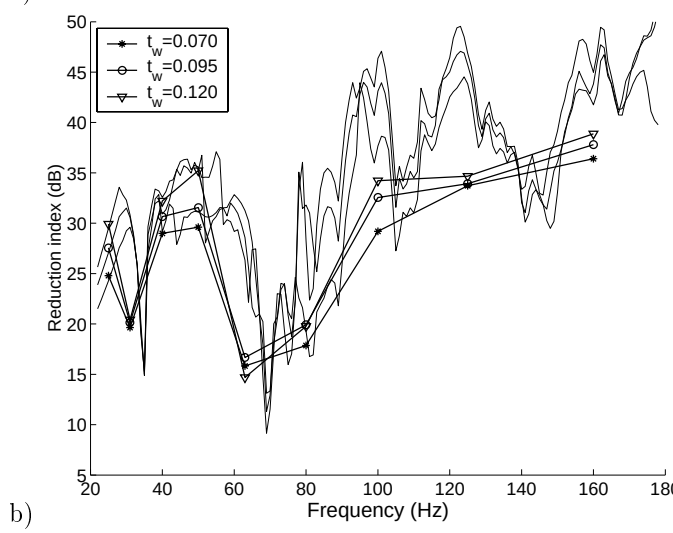

b)

Figure 7: *Reduction index, The effect of wall thickness is evaluated for* t_w *= 0.070, 0.095 and 0.120 m, a) s=0.45 m, b) s=0.60 m.*

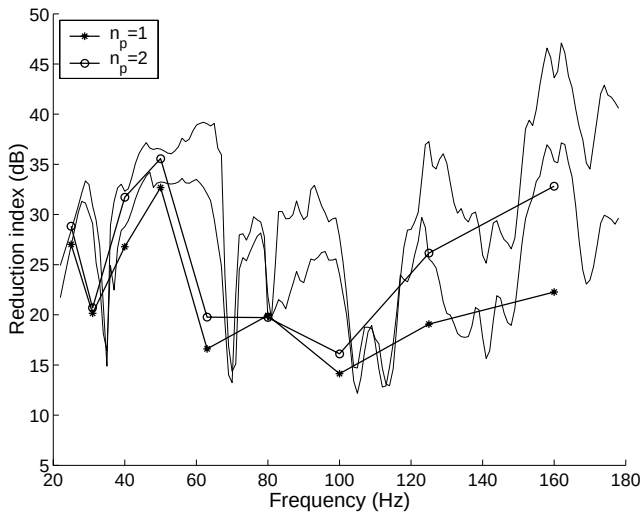

a)

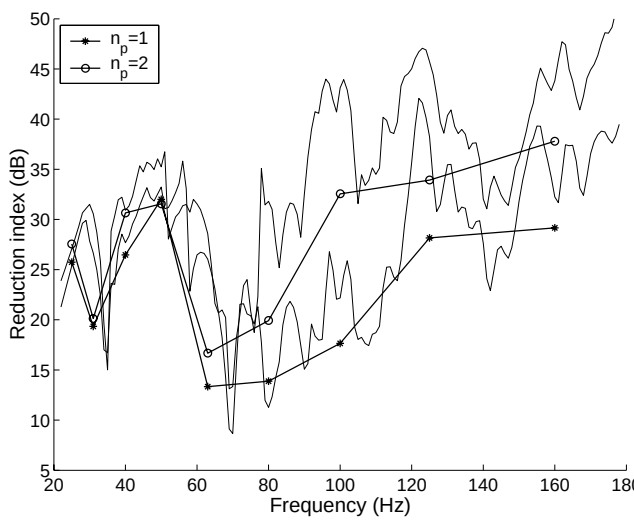

b)

Figure 8: *Sound reduction, the calculations being performed for use of one and of two plaster boards, a) s=0.45 m, b) s=0.60 m.*

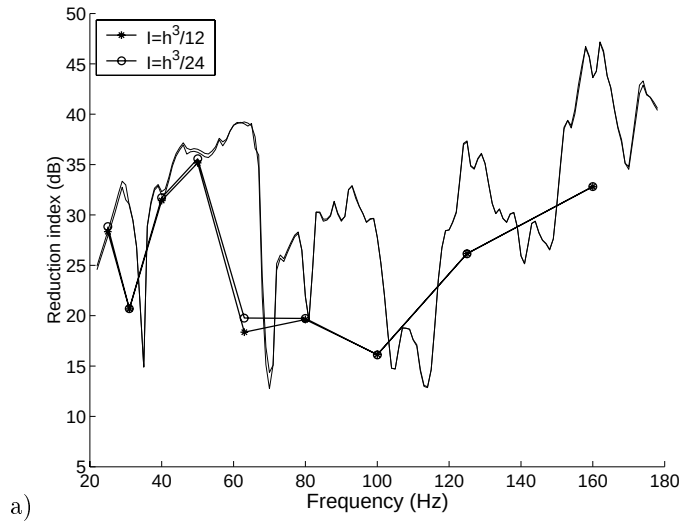

a)

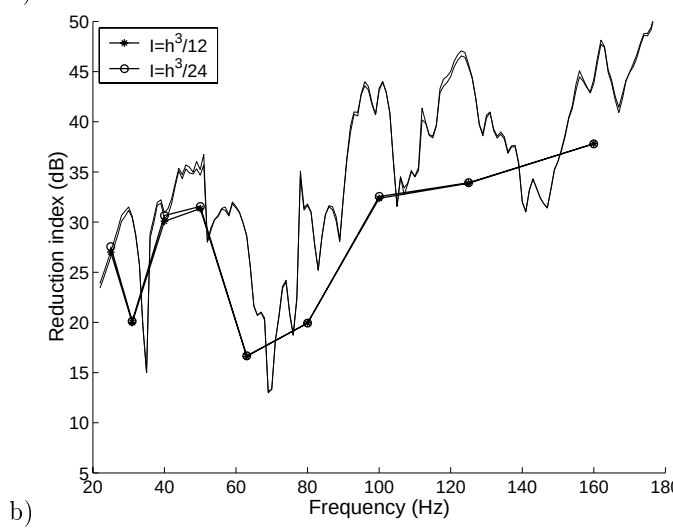

b)

Figure 9: *Sound reduction when the wall stud stiffness is varied in terms of the moment of inertia of the finite elements in the web, being either* $t_{web}^3/12$ *(homogenous section) or* $t_{web}^3/24$*, a) s=0.45 m, b) s=0.60 m.*

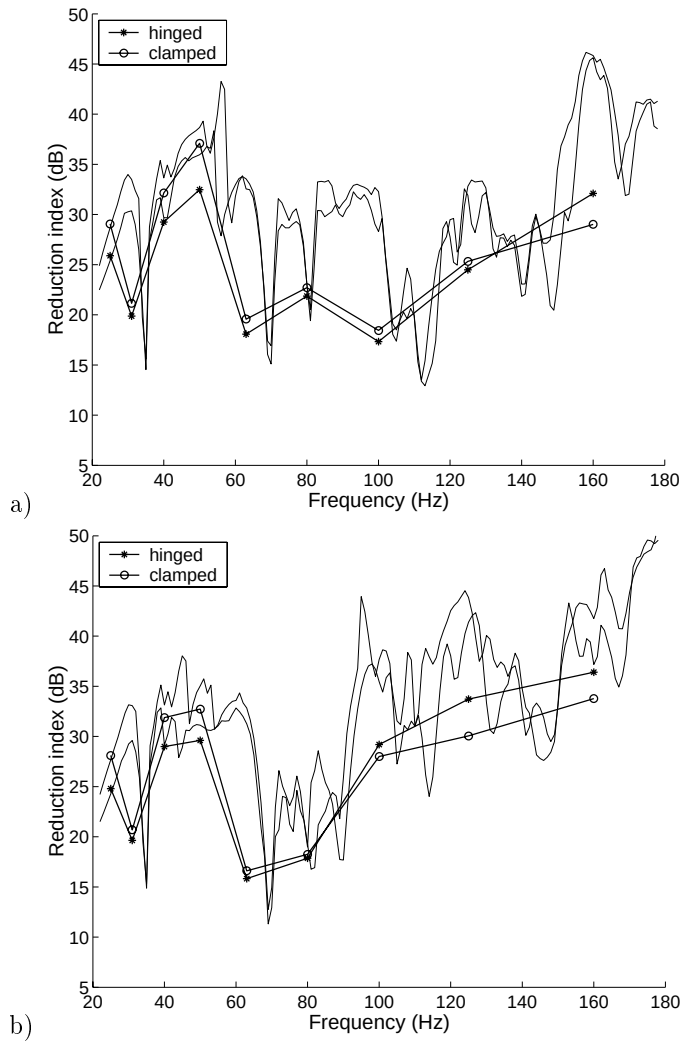

Figure 10: *Sound reduction when the boundary conditions are modelled as being free vs. as being clamped, a) s=0.45 m, b) s=0.60 m.*

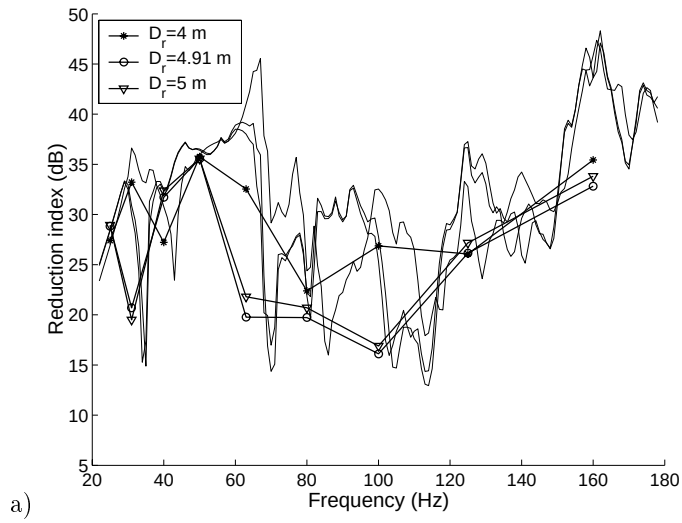

a)

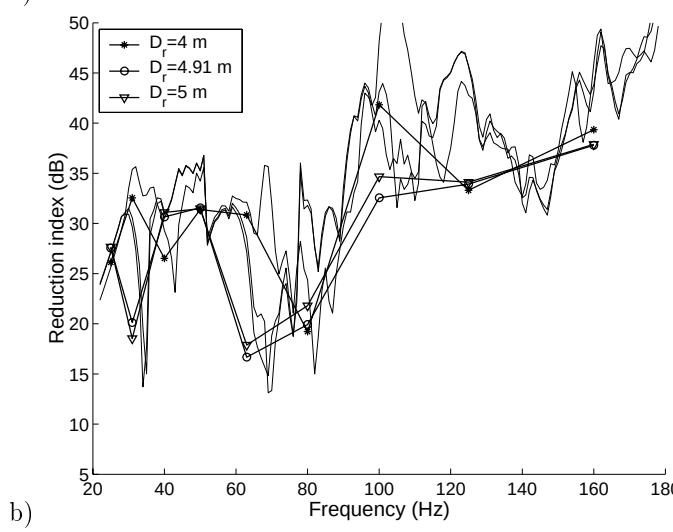

b)

Figure 11: *Sound reduction when the depth of the receiving room perpendicular to the wall that is studied is varied, a) s=0.45 m, b) s=0.60 m.*

4.1 Behavior at the transmission peak

The sound transmission is calculated as being very large in the region of 70 Hz. A frequency response plot showing the sound pressure in the sending and in the receiving room around this frequency is shown in Fig. 12. The sound level in the sending room has peak values at frequencies that match the two coupled modes that are shown in Fig. 13. In the receiving room, the peak level lies between these frequencies and the two coupled modes interact. Fig. 14 presents a plot of the real and the imaginary part of the frequency response at maximum sound transmission. In the area where the microphones are located the magnitude of the pressure level in the two rooms is similar.

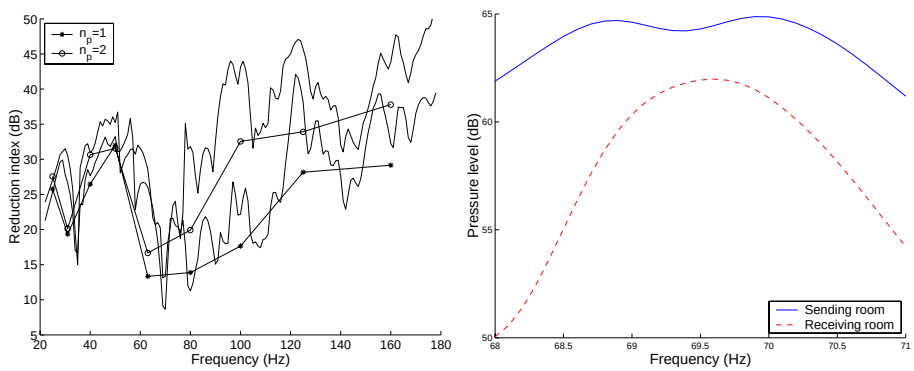

Figure 12: *a) Degree of sound reduction, indicating transmission to be high at 70 Hz, both for single and double plaster boards. b) The sound pressure levels in the sending room and the receiving room, which differ in the frequencies at which peak levels are achieved.*

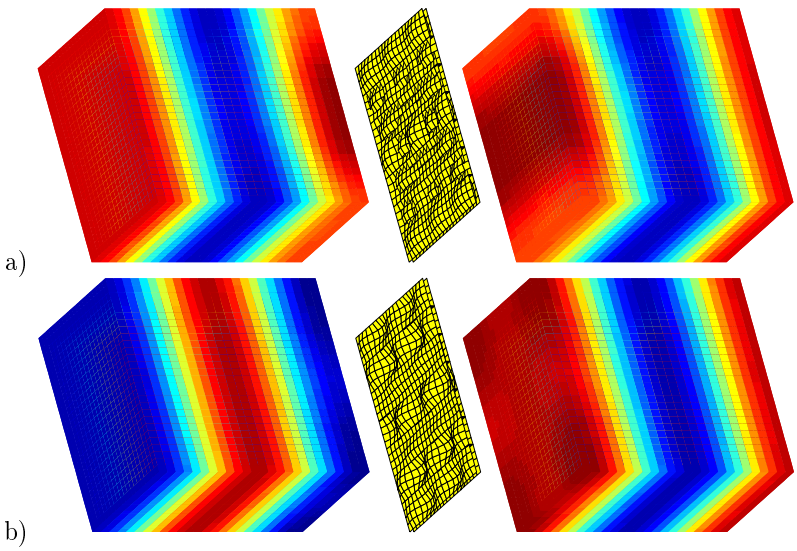

Figure 13: *Coupled modes, a) $f = 68.9$ Hz, b) $f = 69.9$ Hz.*

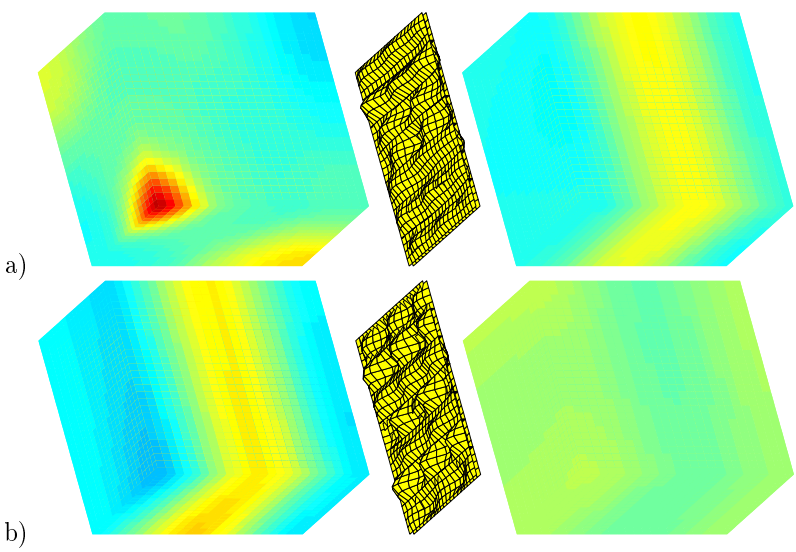

Figure 14: *Frequency response when a point source is applied in the sending room, a) real part, b) imaginary part.*

4.2 Conclusions

The sound reduction of the walls that were studied was determined by finite element analysis. The finite element model provided a description of the basic behavior of the wall, the results being compared with those of the measurements. The parametric study indicated the behavior of the coupled system to be very complex. The expected results in terms of improved sound insulation when the thickness of the wall and the number of plaster boards were increased could be demonstrated. Changing the bending stiffness of the wall stud web or the boundary conditions did not influence the sound reduction to any appreciable extent, however. The dimensions of the sending and the receiving room were found, on the other hand, to have a strong effect on sound transmission. A detailed analysis of the room-wall-room system is needed in order to adequately predict the effect on sound transmission of changes in the properties of the system.

Acknowledgments

The support for this work provided by Lindab Profil AB is gratefully acknowledged.

References

[1] SS-EN ISO 140-3:95. Standard for laboratory measurement of sound reduction of walls (1995).

[2] SS-EN ISO 717-1:96. Standard for evaluation of measured sound reduction (1996).

[3] G. Sandberg, A New Strategy for Solving Fluid-Structure Problems, International Journal for Numerical Methods in Engineering, vol 38, 357-370 (1995).

[4] G. Sandberg, Acoustic and Interface Elements for Structure-Acoustic Analysis in CALFEM, Report TVSM-7113, Lund Institute of Technology, Division of Structural Mechanics, Lund (1996).

[5] K.-G. Olsson, P.-E. Austrell, M. Ristinmaa, G. Sandberg, CALFEM — a finite element toolbox to Matlab, Version 3.2. Report TVSM–9001, Lund Institute of Technology, Division of Structural Mechanics and Department of Solid Mechanics, Lund, Sweden (1999).

[6] A. Pietrzyk, Sound Insulation at low Frequencies, Doctoral thesis, Chalmers Unsiversity of Technology, Department of Applied Acoustics, Göteborg, Sweden (1997).

[7] S. Andreasson. Three-Dimensional Interaction in Stabilisation of Multi-Story Timber Fraame Building Systems, Licentiate thesis, Lund Institute of Technology, Division of Structural Engineering, Lund, Sweden (2000).

[8] M. Sköld. Static analysis of double-leaf walls including the stiffness of the fasteners, TVSM-5108, Lund Institute of Technology, Division of Structural Mechanics, Lund, Sweden (2001).

[9] F. Fahy, Sound and Structural Vibration (Academic Press 1985).

[10] The MacNeal-Schwendler Corporation, MSC/NASTRAN ENCYCLOPEDIA - V70.5, (1998).

[11] The Mathworks Inc., Matlab Reference Guide, (2000).